

Selective Complexation of *N*-Alkylpyridinium Salts: Binding of NAD⁺ in Water

Michael Fokkens,^[a] Christian Jasper,^[a] Thomas Schrader,^{*[a]} Felix Koziol,^[b] Christian Ochsenfeld,^{*[b]} Jolanta Polkowska,^[c] Matthias Lobert,^[c] Björn Kahlert,^[c] and Frank-Gerrit Klärner^{*[c]}

Abstract: A new class of receptor molecules is presented that is highly selective for *N*-alkylpyridinium ions and electron-poor aromatics. Its key feature is the combination of a well-preorganized molecular clip with an electron-rich inner cavity and strategically placed, flanking bis-phosphonate monoester anions. This shape and arrangement of binding sites attracts predominantly flat electron-poor aromatics in water, binds them mainly by π -cation, π - π , CH- π , and hydrophobic

interactions, and leads to their highly efficient desolvation. NAD⁺ and NADP, the important cofactors of many redox enzymes, are recognized by the new receptor molecule, which embraces the catalytically active nicotinamide site and the adenine unit. Even nucleosides such as adenosine

are likewise drawn into the clip's cavity. Complex formation and structures were examined by one- and two-dimensional NMR spectroscopy, Job plot analyses, and isothermal titration microcalorimetric (ITC) measurements, as well as quantum chemical calculations of ¹H NMR shifts. The new receptor molecule is a promising tool for controlling enzymatic oxidation processes and for DNA chemistry.

Keywords: cofactors • host-guest systems • molecular clips • π interactions

Introduction

Many enzymes use NAD⁺ or NADP as cofactors for stereoselective oxidations or reductions. Thus, dehydrogenases catalyze the oxidation of secondary alcohols to carbonyl compounds or the reverse process, decarboxylases facilitate CO₂

extrusion from carboxylic acids, while many more related processes in various biosynthetic pathways all rely on the use of NAD⁺.^[1-4] In the enzyme protein environment the pyridinium unit of NAD⁺ is usually noncovalently buried in a cleft called the Rossman fold.^[5-7] Adenine and nicotinamide are both immersed in cavities with at least one hydrophobic side, facilitated by strong hydrophobic interactions and dispersive forces.^[8] Additional electrostatic interactions and hydrogen bonds with basic amino acids are used to keep the phosphate anions in place. We asked ourselves whether such a microenvironment might be imitated by artificial receptor molecules, which could in turn act as carriers for this important cofactor. To this end we joined our efforts and combined two powerful binding motifs into a new class of synthetic hosts for *N*-alkylpyridinium ions.

State of the art: In recent years the π -cation interaction^[9-12] has been shown to be a major noncovalent force used in numerous proteins.^[13-19] Consequently, theoretical investigations have detailed the electrostatic, hydrophobic and dispersive contributions to this attraction, which works so well in aqueous solution.^[20-23] In the past decade, several groups have designed macrocyclic receptor structures with embedded electron-rich aromatic moieties, which use the π -cation

[a] M. Fokkens, C. Jasper, Prof. Dr. T. Schrader
Fachbereich Chemie der Universität Marburg
35032 Marburg (Germany)
Fax: (+49) 6421-282-5544
E-mail: schradet@staff.uni-marburg.de

[b] Dr. F. Koziol, Prof. Dr. C. Ochsenfeld
Institut für Physikalische Chemie und
Theoretische Chemie der Universität Tübingen
72076 Tübingen (Germany)
Fax: (+49) 7071-295-490
E-mail: christian.ochsenfeld@uni-tuebingen.de

[c] Dr. J. Polkowska, M. Lobert, B. Kahlert, Prof. Dr. F.-G. Klärner
Institut für Organische Chemie
der Universität Duisburg-Essen
45117 Essen (Germany)
Fax: (+49) 201-183-4252
E-mail: frank.klaerner@uni-essen.de

Supporting information for this article is available on the WWW under <http://www.chemeurj.org/> or from the author.

interaction to bind organic cations such as quaternary ammonium ions,^[24–30] guanidinium ions,^[31,32] and *N*-alkylpyridinium ions.^[33–36] However, these macrocyclic structures have a different selectivity towards their substrates; most of them prefer spherical over flat guests.

An alternative approach consists of designing molecular clips that offer a high degree of preorganization and are usually quite selective for flat electron-poor guests. Porphyrin clips derived from diphenylglycoluril have been shown to accommodate *N*-alkylpyridinium cations (e.g., viologen cations) between their tips.^[37] Unfortunately, they also bind to electron-rich aromatics like pyridine, hydroxypyridine, and phenols.^[38] In addition, to date they have been only studied in organic solution.^[37] Three earlier reports have appeared on molecular recognition of NAD⁺ by artificial hosts: Schmidtchen^[39] used a macrocyclic anion receptor to complex the bis-phosphate bridge of NAD⁺. Lehn et al.^[40] presented mono- or bisacridinium-functionalized azacrown ethers, which complex nucleotide anions; a little later, Bianchi et al.^[41] studied azacrowns in their protonated form, which also embrace the diphosphate core of NAD⁺. Cyclic voltammetric measurements indicated significant alterations in the electrochemical behavior of the NAD⁺/NADH couple due to its complexation by the azacrown. However, in all three cases, NAD⁺ complexation mainly involves the interaction of the positively charged host with the diphosphate anion, and not with the catalytically active nicotinamide moiety. This, however, is a major prerequisite for selective interference with dehydrogenases aimed at complexation of their cofactor.

Design: During the past few years Klärner et al. have introduced various molecular tweezers and clips designed for the inclusion of electron-poor guests such as aromatics with –M substituents, pyridinium cations, or even sulfonium cations.^[42] These guests were mainly bound by π – π , CH– π , and π –cation interactions inside their electron-rich concave cavity.^[42] However, due to the lipophilic nature of these hosts, molecular recognition was restricted to organic solvents, mainly chloroform. Introduction of hydrophilic OCH₂CO₂R substituents in the central arene spacer units of the tweezers and clips led to an unfavorable folding of these side chains toward the receptor cavity and prevented efficient binding in polar solution.^[43,44] Schrader et al. have used convergent bis-phosphonate anions extensively for recognition of ammonium alcohol and guanidinium.^[31,32,45] These electron-poor guests are bound by the bis-phosphonate hosts in a chelate arrangement that maximizes electrostatic attraction and establishes at the same time a network of ionic hydrogen bonds. In a joint effort we have now adorned the molecular clip **1** with short phosphonate monoester anions and obtained water-soluble host molecules **1a,b** (Figure 1).^[46] They not only have an open cavity, but they are also flanked by two negatively charged functionalities for additional ion pairing with cationic guests. Molecular modeling studies (molecular mechanics calculations in water, MacroModel 7.1, Amber*)^[47,48] suggested that pri-

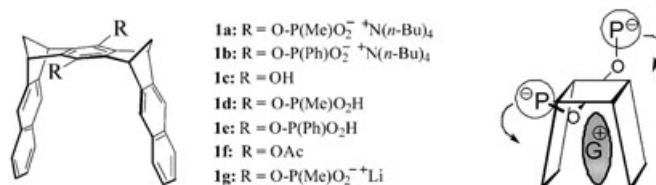
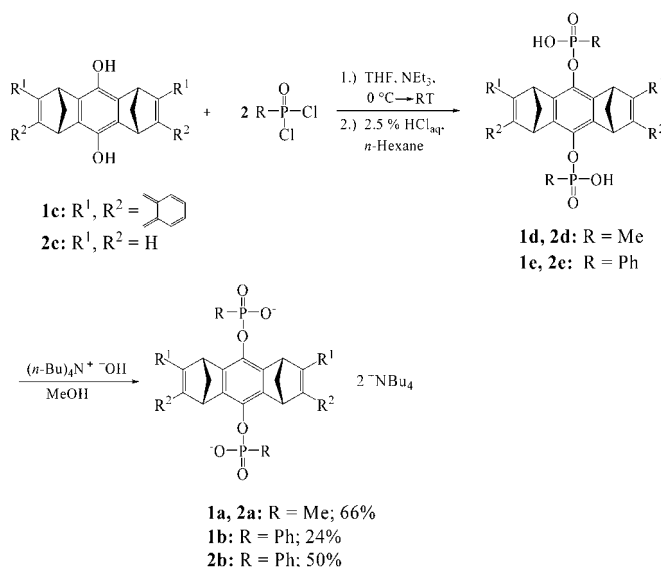


Figure 1. Left: Structures of clips **1a–g**. Right: Schematic design of the new hybrid receptor system as electron-rich molecular clip and bis-phosphonate tweezer.

mary ammonium cations, including ammonium alcohols like adrenaline or aminosugars, should fit into the clip, whereas bulky substituents, as in tertiary and quaternary ammonium salts such as alkaloids or acetylcholine should be rejected.

Results

Synthesis of bis-phosphonate clips 1a,b: The synthesis of **1a,b** followed a straightforward modular strategy (Scheme 1). The deprotonated form of hydroquinone clip **1c**



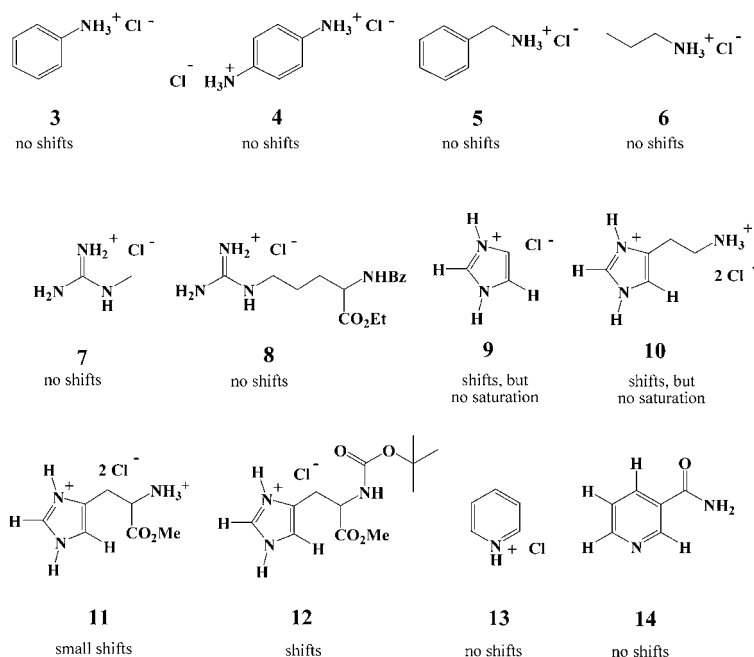
Scheme 1. Synthesis of bis-phosphonate clips **1a** and **1b** and model compounds **2a** and **2b**.

was treated with methyl- or phenylphosphonic acid dichloride, followed by hydrolysis of the remaining chloro substituents. The resulting acids **1d,e** were subsequently deprotonated with a suitable base in a precision titration providing the desired counterion, for example, for maximum solubility. With tetra-*n*-butylammonium counterions, the bis-phosphonate clips **1a,b** are soluble in a wide range of solvents, ranging from chloroform over DMSO and methanol to water. Clips **1a,b** were obtained in good to moderate yields and analytically pure form. In addition to **1a,b** with the whole clip scaffold, two model compounds **2a,b** were synthesized that

lacked the naphthalene side-walls for reasons of comparison. Compounds **2a,b** turned out to be valuable tools for identification of proton-transfer processes and other unspecific binding events.

Binding experiments: The possible self-association of pure clip **1a** in D₂O was investigated by means of the concentration dependence of its ¹H NMR spectrum (Supporting Information: Table S1). No significant changes in the chemical shifts of the clip protons (ca. 0.033 ppm) were observed after dilution of the solution of **1a** by a factor of 32 ([**1a**]=2.70–0.084 mM), and this indicates negligible tendency of clip **1a** for self-association in aqueous solution. However, the larger ¹H NMR downfield shifts found for the NCH₂CH₂ protons ($\Delta\delta=0.138$ and 0.112 ppm) of the tetra-*n*-butylammonium cation in **1a** on dilution is initial evidence for complexation of the cation inside the clip cavity (vide infra).

In preliminary experiments 1:1 mixtures of methylphosphonate clip **1a** and representatives of various classes of organic cations **3–14** were examined for their ability to form host–guest complexes in polar solvents (data for a selection of cations are given in Table 1). The functional groups range



Scheme 2. Potential cationic guest molecules: ammonium salts **3–6**, guanidinium and imidazolium derivatives **9–12** (which may serve as models for basic amino acid side chains), and pyridinium chloride **13**, as well as the neutral nicotinamide **14** are not included into the cavity of clip **1a** in aqueous solution within the limits of ¹H NMR detection.

Table 1. Binding constants K_a [M⁻¹] for 1:1 complexes between primary ammonium salts and the methylphosphonate clip **1a** or phenylphosphonate clip **1b** in various solvents, determined by ¹H NMR titrations at 20 °C.

Guest	K_a (1a , DMSO)	K_a (1b , DMSO)	K_a (1a , MeOD)	K_a (1a , D ₂ O)
aniline·HCl 3	acid–base reaction	–	acid–base reaction	–
benzylamine·HCl 5	2400 ($\pm 8\%$) ^[a]	2100 ($\pm 9\%$) ^[a]	no shifts	–
propylamine·HCl 6	–	6500 ($\pm 44\%$) ^[a]	no shifts	no shifts

[a] The calculated errors represent standard deviations resulting from the curve-fitting procedure. – = not determined.

from aliphatic and aromatic primary ammonium cations over imidazolium and guanidinium ions, to *N*-H, *N*-alkyl-, and *N*-arylpiperidinium or -pyrazinium compounds. In methanol and water, no binding could be observed for any of the ammonium, *N*-H-piperidinium, -imidazolium, or -guanidinium cations shown in Scheme 2. The nonexistent affinity in water or methanol for the piperidinium, imidazolium, and guanidinium cations is surprising in view of their flat nature. We assume that in these cases the displacement of one of the tetra-*n*-butylammonium cations (used as counterion in clip

1a), which is positioned inside the clip cavity in water (vide infra), by one of these cations is energetically not favored. In methanol the phosphonate anions in **1a** are certainly more basic than in water and may deprotonate the *N*-H-ammonium or -iminium groups instead of forming a complex. Since the cations shown in Scheme 2 are the major components in all side chains of basic amino acids, we assume that the new bis-phosphonate clip **1a** does not bind to solvent-exposed amino acid residues on protein surfaces. Control experiments with histidine and arginine derivatives confirmed this assumption: no binding occurs even with the isolated *N*/*C*-protected cationic amino acids **8** and **12** in equimolar amounts with clip **1a** (Scheme 2). Histidine's pronounced tendency for proton transfer renders the evaluation

of the respective binding experiments problematic. Although in both histidine derivatives **10** and **12** considerable shifts occurred in the imidazolium ring, these do not necessarily indicate inclusion inside the cavity. Because of histidine's low pK_a of about 6, dissociation is even observed during dilution, and in unbuffered solution proton transfer to the host releases the free base at the end of most titrations. This even occurred in the binding experiment of **12** with **1a** in a 65-fold excess of buffer (sodium hydrogenphosphate, pH 7). However, since no shifts were observed for

the host, experimental evidence indicates that histidine derivatives are not included in the cavity. Since *p*-xylylene bis-phosphonates have been shown to complex primary ammonium cations in less polar solvents, we checked the ability of clip **1a,b** to recognize these guests in DMSO. This time, moderate chemical shifts were produced in the ¹H NMR signals of the host and guest protons, and well-defined binding isotherms were obtained, which allowed excellent fits for a 1:1 stoichiometry.^[49–51] Job plots in the same solvent confirmed this assumption.^[52–54] The association constants are on the order of 10³ M⁻¹ and agree very well with similar values found for adrenaline derivatives with *p*-xylylene bis-phosphonates. However, in our complexation experiments with clips **1a,b** the maximum complexation-induced shifts $\Delta\delta_{\max}$ remain relatively small (ca. 0.1 ppm) even for the guest protons. Together with the moderate binding constants this makes a strong argument for a purely electrostatic interaction in a chelate binding mode, similar to that already found for xylylene bis-phosphonates in DMSO. Force-field calculations (MacroModel 7.1, Amber*/H₂O)^[47,48] suggest that in these cases the ammonium cation is held by both phosphonate arms above the central benzene ring *syn* to the methylene bridges of the host molecule (Figure 2).

However, as soon as an alkyl or aryl substituent is introduced at the ring nitrogen atom, the resulting permanently charged pyridinium cation is an excellent guest for clip **1a**. Very large complexation-induced shifts $\Delta\delta_{\max}$ of the ¹H NMR guest signals are observed, which reach maximum values of up to +3.5 ppm at saturation. This time, no shifts are observed with the model compounds **2a,b** lacking the naphthalene side walls, so the strong effect must be explained by highly efficient inclusion of the guest molecule in the electron-rich interior of the molecular clips leading to a shielding environment for the aromatic guest protons. The list of representa-

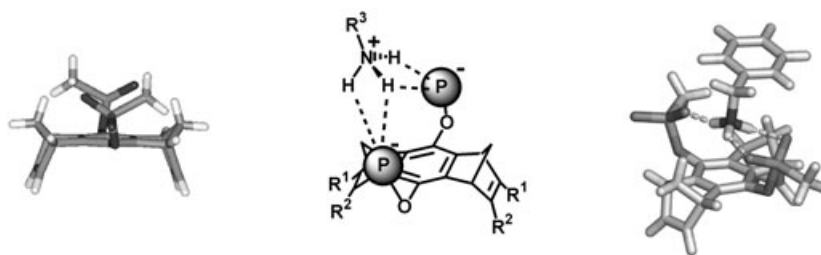
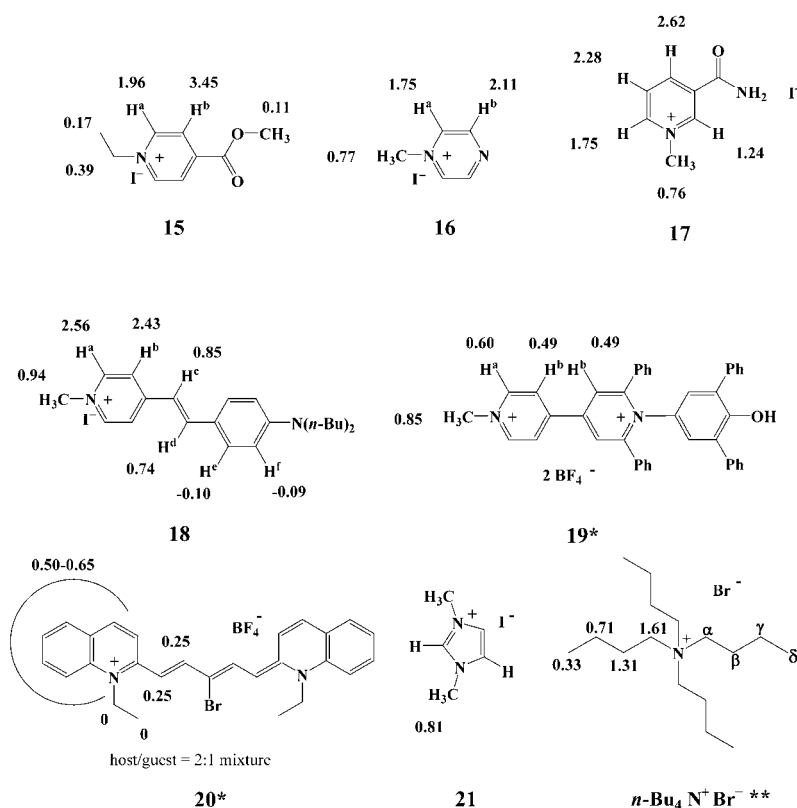


Figure 2. Left: model compound **2a** lacking the side walls (side view). Middle: proposed binding mode for alkylammonium ions by **1** and **2** in DMSO. Right: Monte Carlo simulation of complex **5-2a** in chloroform (MacroModel 7.1, Amber*/H₂O, 1000 steps).^[47,48]

tive substrate structures (Scheme 2) proves that pyridinium cations are generally included into the electron-rich cavity of clip **1a**, irrespective of the substitution pattern or the electronic character of functional groups attached to the heterocycle. But also other types of heterocycles, such as pyrazinium or imidazolium cations **16** or **21** (Scheme 3), form stable complexes with clip **1a**. The complexation of the tetra-*n*-butylammonium cation inside the clip cavity could be detected by the use of the lithium phosphonate clip **1g**.



Scheme 3. Structures of *N*-alkyl- and *N*-arylpyridinium, -pyrazinium, and -imidazolium substrates **15–21** and the maximum complexation-induced ¹H NMR upfield shifts $\Delta\delta_{\max}$ of the guest protons in their 1:1 complexes with clip **1a** in water. **15–17**: simple pyridinium or pyrazinium derivatives; **18–20**: dyes with pyridinium-based chromophores. * In the cases of **19*** and **20*** the complexation-induced ¹H NMR upfield shifts ($\Delta\delta_{\text{obs}}$) are given which were observed in the ¹H NMR spectra of a 1:1 mixture of **1a** and **19** or **20** (each 10⁻³ M) in aqueous solutions. ** In the case of *n*Bu₄N⁺Br⁻ the ¹H NMR titration was performed with the lithium salt **1g** as host.

^1H NMR titrations: The maximum complexation-induced shifts $\Delta\delta_{\text{max}}$, binding constants K_a , and hence the Gibbs enthalpies of association ΔG , were determined by means of ^1H NMR dilution titration experiments, which offer the opportunity to observe the complexation-induced shifts in both components (host and guest) at the same time. They also allow the binding curves to be determined for very stable complexes, which is mostly not feasible by means of “conventional” NMR titration experiments in which either the guest or host concentration is varied, while the concentration of the other component is kept constant. In the initial experiments, already reported in a communication,^[46] we calculated these data by using an iterative nonlinear regression analysis from the dependence of the complexation-induced shifts of the ^1H NMR signals of **1a** $\Delta\delta_{\text{obs}}$ on dilution of the NMR sample containing both host and guest. To obtain comparable results we used the same three receptor signals for each calculation. A comparison of the ^1H NMR spectra of clip **1a** with those of the model compound **2a** and of mixtures of **1a** with various guest molecules indicates, however, strong interactions of the alkyl side chains of the tetra-*n*-butylammonium cation with the arene units of the clip framework in aqueous solution; these interactions are diminished by changing the solvent from D_2O over $\text{D}_2\text{O}/\text{CD}_3\text{OD}$ (1:1) to pure CD_3OD (Table 2). The weak solvent

Table 2. Comparison of the ^1H NMR shifts δ of the tetra-*n*-butylammonium protons of clip **1a**, model compound **2a**, and mixtures of **1a** or **2a** with *N*-methylnicotinamide iodide (**17**) or NAD^+ (**22**).

Compound	Solvent	$\delta(\alpha\text{-CH}_2)$	$\delta(\beta\text{-CH}_2)$	$\delta(\gamma\text{-CH}_2)$	$\delta(\delta\text{-CH}_3)$
1a	D_2O	2.37	0.96	0.96	0.73
	$\text{D}_2\text{O}/\text{CD}_3\text{OD}^{\text{[a]}}$	2.70	1.22	1.14	0.85
	CD_3OD	3.06	1.51	1.32	0.96
1a+17	D_2O	2.86	1.37	1.21	0.87
	$\text{D}_2\text{O}/\text{CD}_3\text{OD}^{\text{[a]}}$	2.94	1.42	1.26	0.91
	CD_3OD	3.21	1.64	1.40	1.01
1a+22	D_2O	2.80	1.32	1.18	0.85
	$\text{D}_2\text{O}/\text{CD}_3\text{OD}^{\text{[a]}}$				
	D_2O	3.17	1.62	1.32	0.91
2a	$\text{D}_2\text{O}/\text{CD}_3\text{OD}^{\text{a)}$	3.20	1.64	1.41	0.98
	CD_3OD	3.20–3.29	1.60–1.74	1.35–1.49	1.03
	D_2O	3.21	1.67	1.38	0.96
2a+22	D_2O	3.22	1.67	1.38	0.97

[a] 1:1 mixture.

dependence of the chemical shifts of the $\text{NCH}_2\text{CH}_2\text{CH}_2\text{CH}_3$ protons in the spectrum of **2a** is a good indicator that these interactions are less important in the model compound **2a** lacking the naphthalene sidewalls.

The pronounced upfield shifts of the $\text{NCH}_2\text{CH}_2\text{CH}_2\text{CH}_3$ protons in the spectrum of **1a** in D_2O suggest that the alkyl side chains of the tetra-*n*-butylammonium cation are partially included into the clip cavity (Figures 3 and 4). This assumption could be confirmed by the finding that the lithium phosphonate clip **1g** forms a stable complex with tetra-*n*-butylammonium bromide in aqueous solution. The association constant ($K_a = 3800 \pm 150 \text{ M}^{-1}$) and the $\Delta\delta_{\text{max}}$ values of the guest signals (Scheme 3) were determined for the formation

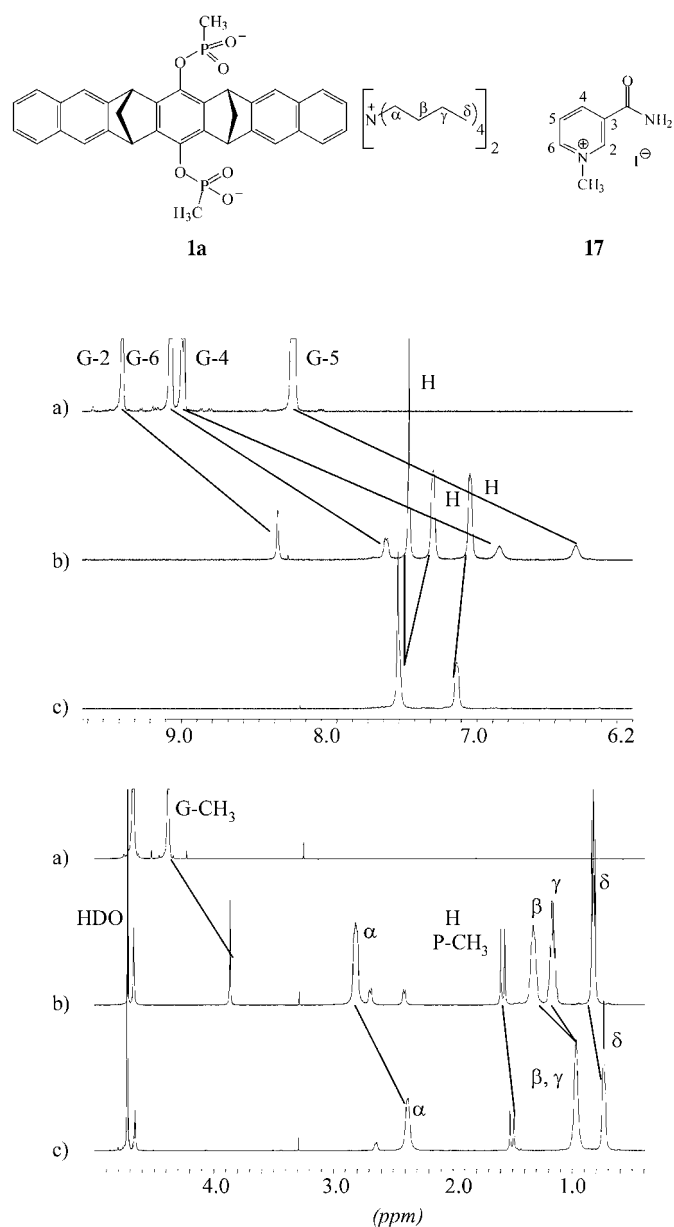


Figure 3. ^1H NMR spectra in the aromatic (top) and aliphatic regions (bottom) of a) **17**, b) mixture of **1a** ($c=9.57 \text{ mM}$) and **17** ($c=9.90 \text{ mM}$), and c) clip **1a** in D_2O at 25°C .

of this complex in water by ^1H NMR dilution titration. Addition of an equimolar amount of *N*-methylnicotinamide (**17**) to a solution of tetra-*n*-butylammonium phosphonate clip **1a** in D_2O leads to a substantial downfield shift of the signals assigned to the *n*-butyl protons and to an even more substantial upfield shift of the signals assigned to the protons of **17** (relative to signals found in the spectra of pure **1a** and pure **17**). This finding allows us to conclude that **17** is indeed included in the clip cavity by replacing the tetra-*n*-butylammonium cation, that is, it forms the more stable complex. Similar results were obtained when NAD^+ (**22**) was added to a solution of **1a** in D_2O (Figures 3 and 5, Table 2). The addition of tetra-*n*-butylammonium bromide

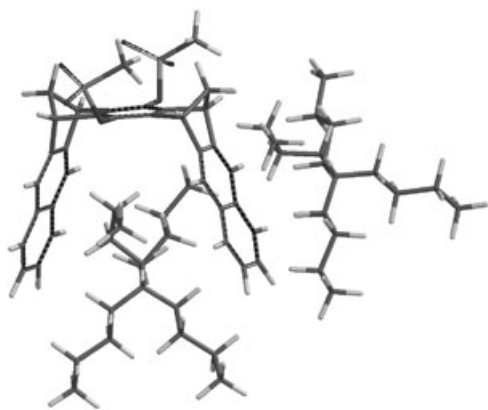


Figure 4. Structure of **1a** calculated by a Monte Carlo conformer search (5000 structures, AMBER*/H₂O, MacroModel 6.5^[47,48]).

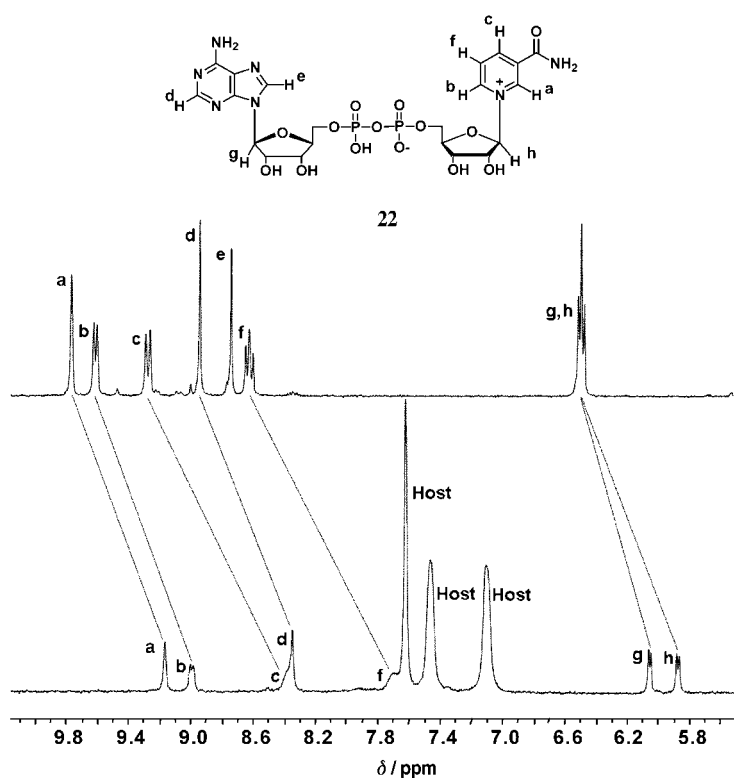


Figure 5. ¹H NMR spectra (aromatic region) of NAD⁺ (**22**) before and after addition of clip **1a** in water. Note the strong upfield shifts of the pyridinium protons a and b, c and f as well as the diverging behavior of both anomeric protons g and h upon complexation. (See above Lewis structure for the assignment of the guest protons.)

(0.5 M) to an aqueous solution of the complex between clip **1a** and *N*-methylnicotinamide iodide ($[\mathbf{17}\cdot\mathbf{1a}] = 10^{-4}$ M) leads to a complete dissociation of this complex within the limits of ¹H NMR detection. Evidently, the tetra-*n*-butylammonium cation in high concentration can again displace the *N*-methylnicotinamide cation in the complex with **1a**, although it binds more weakly to **1a**.

Further support for the close spatial contact between the clip framework and the butyl groups of the ammonium cat-

ions in **1a** came from two-dimensional NOESY experiments. In spectra of both **1a** and a 1:1 mixture of **1a** and **17** in D₂O, intense cross-peaks between the signals of the NCH₂CH₂CH₂CH₃ protons and all of the clip protons indicate close spatial contacts between these protons. In D₂O/CD₃OD none of these cross-peaks can be detected any more. Apparently, methanol solvates both species individually, and the solvent shells prevent their close spatial approach, which is necessary to observe the nuclear Overhauser effect. (The NOESY spectra are shown in the Supporting Information.)

The complexation-induced shifts $\Delta\delta_{\text{obs}}$ of the ¹H NMR signals of the guest protons were used to determine the K_a and $\Delta\delta_{\text{max}}$ values from the binding curves, because the larger shifts of these signals make them a more sensitive probe for complex formation than the host signals. In addition to the good fit of the binding isotherms, Job plots confirmed the assumed 1:1 stoichiometry of the inclusion complexes. Figure 6 shows the binding curves and the Job plot analysis

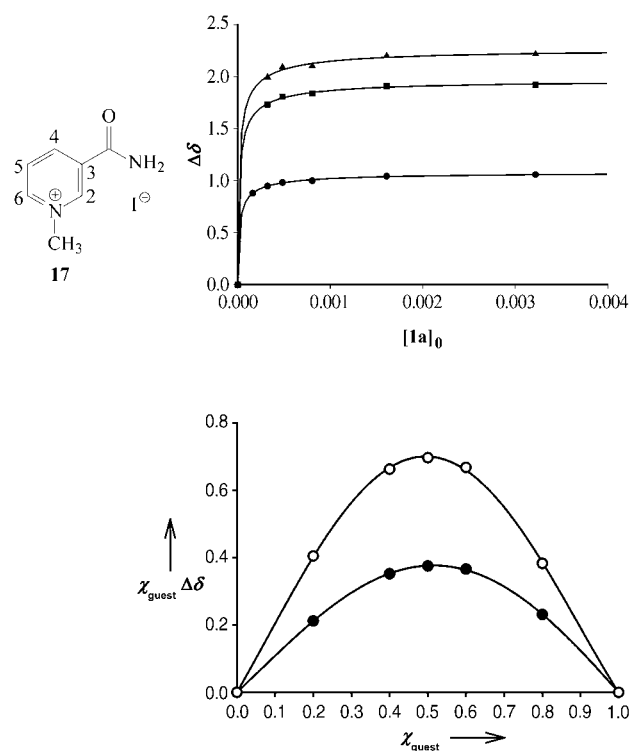


Figure 6. Top: ¹H NMR dilution titration curves for complex formation between **1a** and *N*-methylnicotinamide (**17**) showing the dependence of the complexation-induced shifts $\Delta\delta$ of protons 2-H (●), 4-H (▲), and 5-H (■) of **17** in D₂O. Bottom: Job plot for complex formation between **1a** and **17** in CD₃OD, shown for the guest protons 2-H (●) and 5-H (○); χ = mole fraction.

for complex formation between clip **1a** and *N*-methylnicotinamide (**17**). The complex **1a**·**17** is by far the most stable one, since many of the experimental points lie in the saturation region of the curve (Figure 6). In this case the experimental error is certainly larger than the standard deviation, and the K_a value given in Table 3 is only a lower limit. The

Table 3. Association constants K_a and Gibbs enthalpies of association ΔG for complex formation between clip **1a** and guest molecules **17–26**, determined by ^1H NMR dilution titration in methanol and water at 20°C .

Substrate	K_a [M^{-1}] ^[a,b] in CD_3OD	$-\Delta G$ [kcal mol $^{-1}$]	K_a [M^{-1}] ^[a,b] in D_2O	$-\Delta G$ [kcal mol $^{-1}$]
nicotinamide (17)	17250 ± 1950	5.8	83000 ± 9400	6.7
Kosower salt (15)	4300 ± 450	4.9	4800 ± 1300 ^[c]	4.9
pyrazinium salt (16)	600 ± 30 ^[c]	3.8	10000 ± 2500	5.3
pyridinium dye (18)	2950 ± 300	4.7	broad signals ^[d]	–
imidazolium salt (21)	–	–	7900 ± 1700	5.2
NAD^+ (22)	precipitation ^[d]	–	9100 ± 3450	5.4
NADP (23)	–	–	3900 ± 400	4.8
2'-desoxyadenosine (24)	–	–	5300 ± 320	5.0
AMP (25)	–	–	1100 ± 200	4.0
NMN (26)	–	–	6800 ± 1500	5.1

[a] Determined from the complexation-induced ^1H NMR shifts of the guest proton signals. [b] The given errors are standard deviations between the K_a values from different NMR signals; the standard deviations from the nonlinear regressions were consistently lower. [c] Determined from host signals. [d] Precipitation of the complex after mixing **1c** and **22** and broad signals in the ^1H NMR spectrum of a mixture of **1c** and **18** prevent the determination of K_a .

results obtained for the complexation of various *N*-alkyl- or *N*-arylpyridinium, *N*-alkylpyrazinium, and *N*-alkylimidazolium cations with clip **1a** are summarized in Table 3 (K_a and ΔG values) and in Schemes 3 and 4 ($\Delta\delta_{\text{max}}$ values). Remarkably, neutral guests like 2'-desoxyadenosine (**24**) also form rather stable complexes with **1a**.

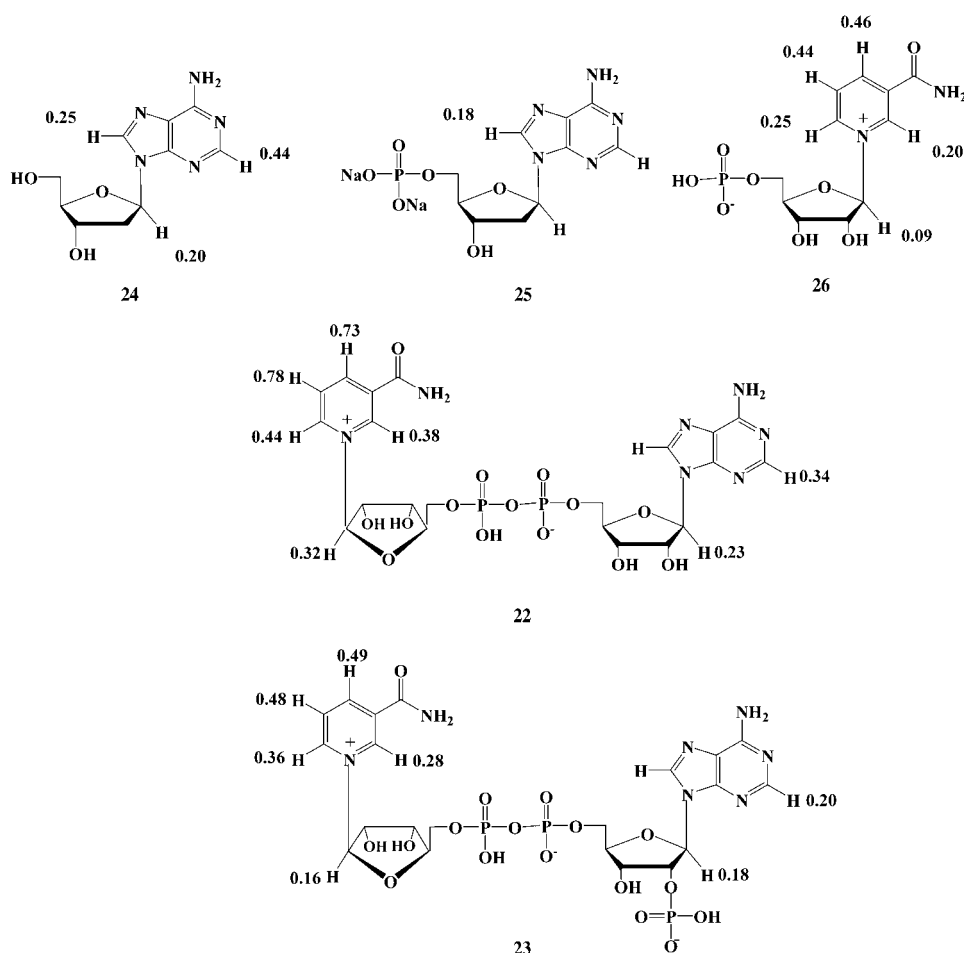
Mass spectrometric analysis:

The complexes of clip **1a** can be also detected by mass spectrometry. Strong molecular ion peaks for these complexes appeared in the ESI-MS spectra (negative ions). Figure 7 shows the ESI-MS spectrum of the complex between clip **1a** and 2'-desoxyadenosine (**24**) as an example. Although the complex of **1a** with NAD^+ (**22**) was only sparingly soluble in $[\text{D}_4]$ methanol, the supernatant solution produced a clean ESI spectrum, which showed peaks for both the free host **1a** and its 1:1 complex with the fully deuterated guest **22**.

Calorimetric titrations: Isothermal titration microcalorimetry (ITC) is frequently applied for the quantification of the enthalpy and entropy changes ΔH and ΔS resulting from complex formation.^[55] We used ITC to study complex formation be-

tween clip **1a** and *N*-methylnicotinamide (**17**) or NAD^+ (**22**). From the sign of the heat pulses produced during the titration of the aqueous guest solution to an aqueous clip solution it is immediately apparent that host–guest binding in both systems is exothermic. Both titration curves, however, exhibit unusual, but reproducible, shapes (Figures 8 and 9). In the case of **17** and **1a**, no plateau was found at the beginning of the titration, and the curve (even after correction for the heats of dilution) cannot be fitted with the 1:1 complex stoichiometry that was found by

Job plot analysis. Regression analysis of the experimental data with stoichiometry factor n as an additional variable parameter leads to a good fit for $n = 0.889$ (Figure 8). We re-



Scheme 4. Nucleosides and nucleotides (NAD^+ derivatives) **22–26** bound by the clip **1a** and the maximum complexation-induced ^1H NMR upfield shifts $\Delta\delta_{\text{max}}$ of the guest protons in their 1:1 complexes with clip **1a** in water.

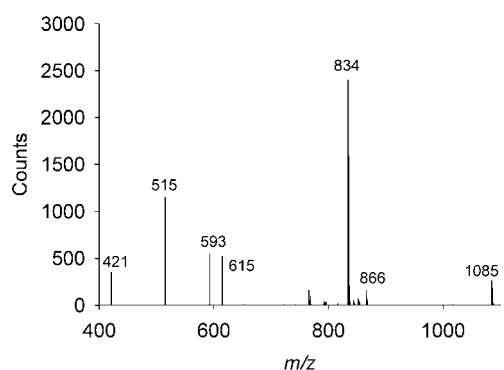


Figure 7. ESI-MS spectrum for the complex between clip **1a** and 2'-desoxyadenosine (**24**). The spectrum was recorded in the negative ion mode. The calculated masses are: $[\mathbf{1a}+\mathbf{24}]^{2-}$: 421; $[\mathbf{1a}-\text{OPOMe}]^{-}$: 515; $[\mathbf{1a}+\text{H}^+]^{-}$: 593; $[\mathbf{1}+\text{Na}^+]^{-}$: 615; $[\mathbf{1a}+(\text{nBu})_4\text{N}^+]^{-}$: 834; $[\mathbf{1a}+\mathbf{24}+\text{Na}^+]^{-}$: 866; $[\mathbf{1a}+(\text{nBu})_4\text{N}^+] + \mathbf{24}]^{-}$: 1085. No ion peaks were found beyond $m/z = 1100$.

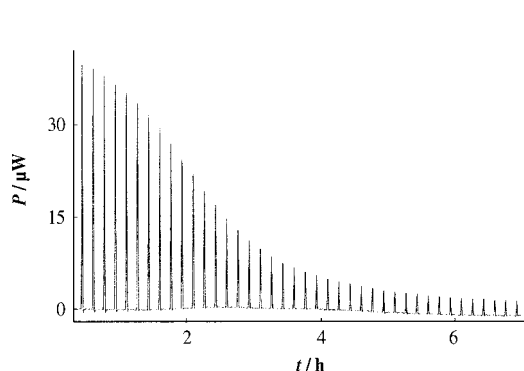


Figure 8. Top: Plot of the heat pulses measured during the titration of **1a** with **17** in H_2O ($[\mathbf{1a}] = 819 \mu\text{M}$, $[\mathbf{17}] = 5723 \mu\text{M}$). Bottom: The fit from the iterative regression analysis of this plot for the stoichiometry factor $n = 0.889$.

peated the ITC measurements several times using different starting concentrations $[\mathbf{1a}]$ and $[\mathbf{17}]$. The stoichiometry factor n varied in the range from 0.856 to 0.889, and the apparent association constants K_a derived from the fits of these curves are substantially smaller ($1390\text{--}5340 \text{M}^{-1}$) than that obtained from the ^1H NMR titration experiment. The K_a values obtained from the ITC measurements are only valid for stoichiometry factors $n < 1$ (Supporting Informa-

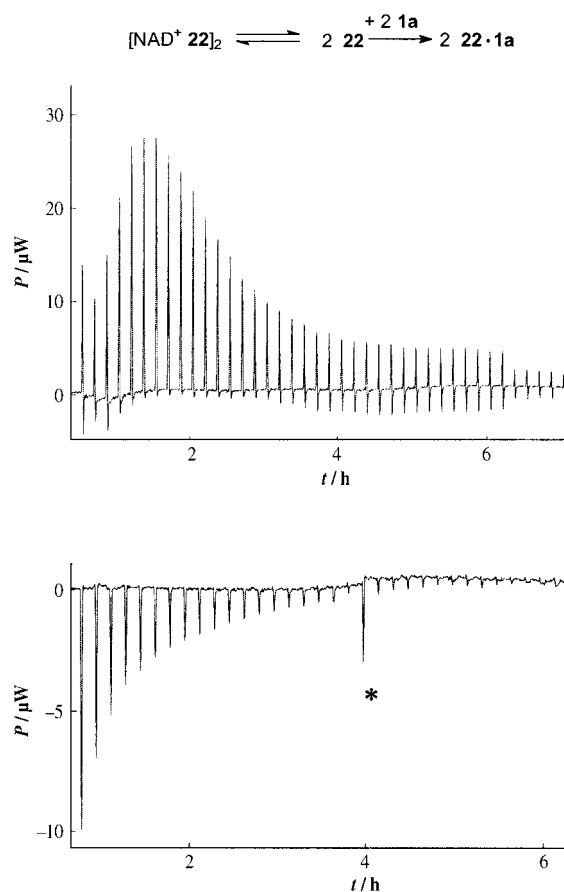


Figure 9. Top: Plot of the heat pulses measured during the titration of **1a** with **22** in H_2O ($[\mathbf{1a}] = 832 \mu\text{M}$, $[\mathbf{22}] = 7610 \mu\text{M}$). Bottom: Heat of dilution of **22**; 40 $10 \mu\text{L}$ portions of a solution of **22** ($7610 \mu\text{M}$) in H_2O were added to 1 mL of H_2O . * artefact of the measurement.

tion, Table S3) and not for formation of the 1:1 complex. The discrepancy between the NMR and ITC measurements can be explained as follows: At the beginning of the ITC experiment there is a large excess in the host concentration, so that formation of a 2:1 host–guest complex is favored. As the titration progresses, the guest concentration increases and the more stable 1:1 complex is formed. The combination of these two processes taking place during the titration explains why the stoichiometry factor is smaller than unity ($n < 1$). In the case of the NMR dilution experiment, we start from a nearly 1:1 mixture of host and guest and therefore the formation of a 2:1 complex is highly unlikely. Fractional stoichiometry factors have been also observed in other ITC measurements on host–guest interactions.^[56,57] The solubility of clip **1a** in water is, however, too low to carry out a reverse ITC titration. This experiment, in which a saturated solution of the clip ($[\mathbf{1a}]_0 = 0.001 \text{M}$) in water was added to *N*-methylnicotinamide iodide ($[\mathbf{17}]_0 = 0.000012 \text{M}$), produced only heat pulses that were not significantly larger than those obtained by dilution of a solution of **1a** in pure water.

The heat pulses evolved at the beginning of the titration of an aqueous solution of **1a** with an aqueous solution of

NAD⁺ (**22**) are smaller than those after the addition of several portions of **22**, and they pass through a maximum before decreasing. At first glance, this is surprising and not expected for a simple host–guest binding (Figure 9, top). Independent measurement of the heat of dilution of **22** in water shows, however, that **22** forms a self-aggregate in aqueous solution which must be dissociated before the complex **22·1a** can be formed. According to the heat of dilution measured by ITC, the dissociation of the self-aggregate of **22** is an endothermic process (Figure 9, bottom), which must be overcompensated by the exothermic complex formation between dissociated **22** and **1a**. We evaluated the two plots shown in Figure 9 under the assumption that the self-aggregate of **22** is a dimer and dissociates prior to complex formation according to the equation in Figure 9. Neglecting the first five heat pulses measured in the titration of the aqueous solution of **22** to that of **1a** leads to the thermodynamic parameters for the formation of the 1:1 complex **22·1a** given in Figure 10. The binding constant $K_a = 8800 \pm 500 \text{ M}^{-1}$ derived from the ITC measurements is in good agreement with that determined by ¹H NMR titration (Table 3).

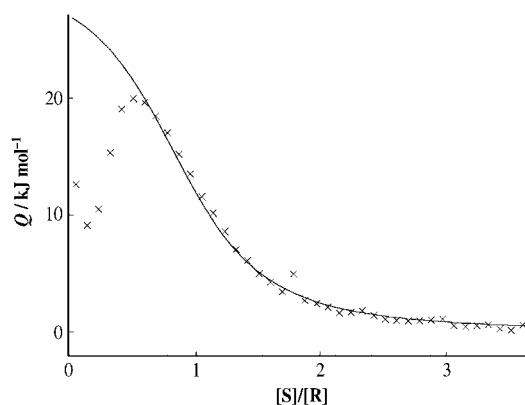


Figure 10. The fit from the iterative regression analysis evaluating the plots shown in Figure 9 by means of the stoichiometry factor $n=1.0$ results in the enthalpy, entropy, and Gibbs enthalpy of association $\Delta H = -7.3 \pm 0.1 \text{ kcal mol}^{-1}$, $\Delta S = -6.7 \pm 0.5 \text{ cal mol}^{-1} \text{ K}^{-1}$, $\Delta G = -5.4 \pm 0.1 \text{ kcal mol}^{-1}$, and the association constant $K_a = 8800 \pm 500 \text{ M}^{-1}$.

Discussion

Complex stabilities: In contrast to complexes of dimethylene-bridged clips of type **1** in aprotic organic solvents,^[58] clip **1a** forms highly stable complexes with the *N*-alkylpyridinium and -imidazolium salts **15–21**, NAD⁺ (**22**), NADP (**23**), 2'-desoxyadenosine (**24**), AMP (**25**), and NMN (**26**) in protic solvents such as methanol and water (Table 3). For example, Kosower salt **15** forms a substantially more stable complex with clip **1a** in D₂O ($K_a = 4800 \pm 1300 \text{ M}^{-1}$, $\Delta G = -4.9 \text{ kcal mol}^{-1}$) than with the corresponding diacetoxysubstituted clip **1f** in CDCl₃ ($K_a = 137 \pm 14 \text{ M}^{-1}$, $\Delta G = -2.9 \text{ kcal mol}^{-1}$).^[44] This result and the finding that the complexes of **1a** formed in water ($K_a = 4800\text{--}83000 \text{ M}^{-1}$) are

more stable than the corresponding ones in methanol ($K_a = 600\text{--}17250 \text{ M}^{-1}$) are good evidence for a substantial contribution of a hydrophobic effect, besides the cation– π interaction and salt bridges in the receptor–substrate binding processes observed here.^[59] A computational study^[9] predicts that, especially in water, the cation– π interaction should be even more important than the salt bridges and thus largely responsible for the complex stabilities.

The binding of NAD⁺ (**22**) and NADP (**23**), which are the most important redox coenzymes in nature, to clip **1a** is particularly remarkable. In methanol the complex **22·1a** precipitated. In water (or methanol:water 1:1) no precipitation occurred, and distinct upfield shifts were observed in the ¹H NMR signals arising from the protons of the nicotinamide subunit as well as in the adenine nucleoside of NAD⁺ (**22**). These findings unambiguously indicate the complex formation between both subunits of NAD⁺ (**22**) and clip **1a**. Similar results were obtained for the binding of NADP **23** to clip **1a** (Table 3, Scheme 4). The binding constant ($K_a = 9100 \pm 3450 \text{ M}^{-1}$) determined for complex **22·1a** is substantially smaller than that of **17·1** ($K_a = 83000 \pm 9400 \text{ M}^{-1}$), although both guests are *N*-alkylnicotinamide derivatives. There are two reasons which may explain this difference in the complex stability:

- 1) The ribose unit of **22** is bound to the nicotinamide moiety by a tertiary carbon atom in the *N,O*-acetal, which may cause an additional steric hindrance in the complex. This effect should also influence the stability of the complex between NADP (**23**) and **1a**.
- 2) According to ITC measurements NAD⁺ **22** forms a dimer in aqueous solution, and in the process of complexation the equilibrium between dimeric and monomeric **22** must be shifted toward the monomeric form, which leads to a smaller K_a value.

The aggregation of NAD⁺ **22** in water observed by ITC measurements could not be detected by ¹H NMR spectroscopy. Dilution of a solution of **22** in D₂O by a factor of 32 (from 28 to 0.9 mM, Supporting Information, Table S2) led to a shift of the ¹H NMR signals by less than 0.09 ppm. Small shifts of the ¹H NMR signals have been observed in the dilution of aqueous NADP (**23**) by a factor of 20 (from 2.6 to 0.13 mM), and this suggests an aggregation of **23** in water comparable to that of **22**. ITC measurements with NADP are planned to confirm this suggestion.

Extension of the guest profile: The upfield shifts observed in the pyrimidine ring of adenine on binding of NAD⁺ (**22**) and NADP (**23**) by clip **1a** gave a first hint at the possible inclusion of nucleosides. We checked this interesting hypothesis with the naturally occurring nucleosides 2'-desoxyadenosine (**24**) and adenosine monophosphate AMP (**25**). A remarkably high binding constant of $K_a = 5300 \pm 300 \text{ M}^{-1}$ was determined for complex formation between the neutral guest molecule **24** and clip **1a** from the ¹H NMR titration curve. The significantly smaller binding constant obtained

for the complex between negatively charged **25** and clip **1a** ($K_a = 1100 \pm 200 \text{ M}^{-1}$) indicates that the interaction between the negatively charged AMP phosphate and clip phosphonate groups in the complex **24-1a** is repulsive and leads to weakening of the complex. To compare the contributions of the nicotinamide with the adenine subunit we cut the NAD^+ molecule into two halves, each carrying a ribose monophosphate unit. Intriguingly, the binding constant for nicotinamide mononucleotide (NMN, **26**, $K_a = 6800 \pm 1500 \text{ M}^{-1}$) is significantly higher than that of adenosine monophosphate (AMP, **25**, $K_a = 1100 \pm 200 \text{ M}^{-1}$). This observation is further good evidence that in the complexes **22-1a** and **23-1a** both ring systems, that is, the nicotinamide and adenine units, are included in the clip cavity. According to the different binding constants of the complexes **25-1a** and **26-1a**, preferential inclusion of the nicotinamide ring of NAD^+ (**22**) or NADP (**23**) in the cavity of clip **1a** is expected.

Electrostatic potential surface (EPS) calculations were used to explain why the clips of type **1**, analogous to the structurally related tweezers,^[42] selectively bind electron-deficient guest molecules in organic solvents such as chloroform. The EPS of bis-phosphonate clip **1a** is calculated by AM1 to be more negative on the concave face than that of the corresponding parent clip **1** or diacetoxy-substituted clip **1f**. This result can certainly provide an explanation of why **1a** is found to be such a good binder to the strongly electron-deficient cationic guest molecules investigated here. The comparative binding study of NAD^+ and truncated versions thereof (**22-26**) shows, however, that in aqueous solution the complementary host and guest EPS, which is calculated for the isolated molecules in the gas phase (Figure 11), is less important for complex formation in aqueous solution. If the electrostatic host-guest interaction is predominant for complex formation, only the nicotinamide

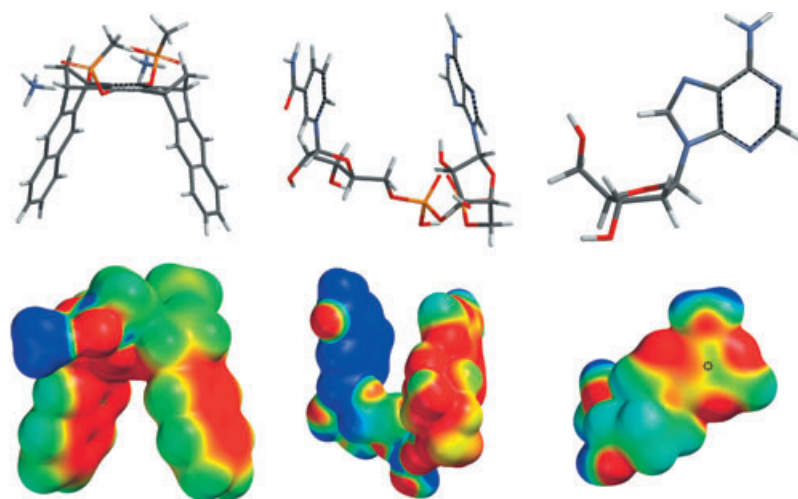


Figure 11. Structure (top) and electrostatic potential surface (EPS, bottom) of clip **1a** with $(\text{NH}_4^+)_2$ instead of $(\text{NBu}_4^+)_2$ as counterions (left), NAD^+ (**22**, middle), and 2'-desoxyadenosine (**24**, right) calculated by AM1. The color code spans from -25 (red) to $+25 \text{ kcal mol}^{-1}$ (blue). The clip geometry was optimized by AM1, whereas in the case of NAD^+ a single-point AM1 calculation was performed using the NAD^+ geometry obtained from the Monte Carlo conformer search of the complex **22-1a** (Figure 16, bottom). Note that the EPS of the nicotinamide subunit in **22** is highly positive compared to that of the adenine moiety.

ring and not the adenine moiety of **22-26** should be bound to the clip cavity according to the large difference in the EPS of the nicotinamide and adenine units shown in Figure 11. Therefore, besides the electrostatic interactions other effects such as the hydrophobic effect seem to be important for the strong binding of clip **1a** to the various guests in aqueous or methanolic solution reported here.^[59-63]

Complex structures: The maximum complexation-induced ^1H NMR shifts of the substrate signals $\Delta\delta_{\text{max}}$ are a very sensitive probe of the complex structures. The large $\Delta\delta_{\text{max}}$ values determined for the pyridinium cations **15-20** (Scheme 3) in their complexes with **1a** are a good indicator that the guest molecules are positioned inside the clip cavity and experience the magnetic anisotropy of the host arene units. The comparison of the $\Delta\delta_{\text{max}}$ values of the Kosower salt **15** in the complexes with clip **1a** ($\Delta\delta_{\text{max}} = 1.96$ (H^a), 3.45 (H^b)) and with diacetoxy-substituted clip **1f** ($\Delta\delta_{\text{max}} = 1.82$ (H^a), 2.40 (H^b)) shows that the complex structures are similar and independent of the substitution pattern at the central spacer unit of the clip. According to the single-crystal structure analysis of the 1:1 complex between *N*-ethyl-4-carboxypyridinium triiodide (a derivative of **15**) and **1f** (Figure 12), the naphthalene sidewalls of the clip embrace the guest molecule tightly by reducing the distance between the naphthalene tips from 10 to 8 \AA .^[58] Provided the complex structures in the crystal and in solution are similar, the observation of only one ^1H NMR signal for the nonequivalent guest protons H^a , $\text{H}^{a'}$, or H^b , $\text{H}^{b'}$ of **15** or **16** in the complexes with clip **1a** indicates that exchange of these protons by rotation of the guest molecule inside the clip cavity and/or by mutual host-guest dissociation/association is fast with respect to the NMR timescale.

The complex between the dye **18** and clip **1a** provides some information about the selectivity of **1a** toward guest structures. In the complex **18-1a**, the NMR signals arising from the pyridinium ring protons exhibit large upfield shifts, whereas the positions of the signals of the protons of the amino-substituted benzene moiety remains almost unchanged, that is, only the pyridinium ring is included inside the cavity of **1a**. In all examined pyridinium and amidinium dyes (**18-20**), no change in color or UV/Vis extinction maxima are found, although NMR data clearly reveal their inclusion within the naphthalene side walls of the cavity. Evidently, the sandwich complex does not lead to charge transfer between host and guest aromatics.^[64]

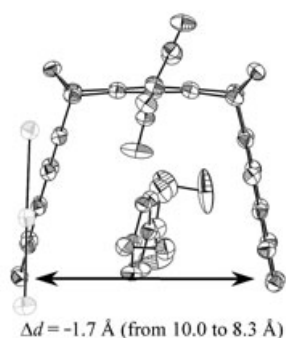


Figure 12. Single-crystal structure of the complex between *N*-ethyl-4-carboxypyridinium triiodide and diacetoxy-substituted clip **1f**.^[58]

In the ^1H NMR spectra of the complexes **22-1a** and **23-1a**, the signals arising from the protons of both subunits (nicotinamide and adenine moieties) are shifted upfield. This observation already allows us to conclude that each complex must exist in at least two conformations in which either the nicotinamide or the adenine subunit is included inside the cavity of **1a**. Accordingly, the two conformations must equilibrate rapidly on the NMR timescale, so that only averaged $\Delta\delta_{\text{max}}$ values are observed. The $\Delta\delta_{\text{max}}$ values determined for the guest protons in the complexes **24-1a**, **25-1a**, and **26-1a** are of similar magnitude to those of the NAD and NADP complexes **22-1a** and **23-1a**. The upfield shifts of the signals of the complexed nicotinamide protons in **22-1a**, **23-1a**, and **26-1a** are significantly smaller than in **17-1a**. This indicates that the nicotinamide rings of **22**, **23**, and **26**, each attached to a ribose unit, are positioned inside the clip cavity differently to the nicotinamide moiety of **17**, which is attached to a methyl group. To gain further insight into this structural problem we performed quantum chemical ^1H NMR shift calculations.

Quantum chemical calculations for *N*-methylnicotinamide complex 17-1a: The host-guest complex of *N*-methylnicotinamide **17-1a** (NMNA for short) was investigated with quantum chemical methods. In a first step, possible lowest energy structures were determined by performing a Monte Carlo conformer search at the force-field level (Amber*/H₂O; MacroModel 6.5; Figure 13).^[47,48] Investigation of the influence of the tetra-*n*-butylammonium cations at this level

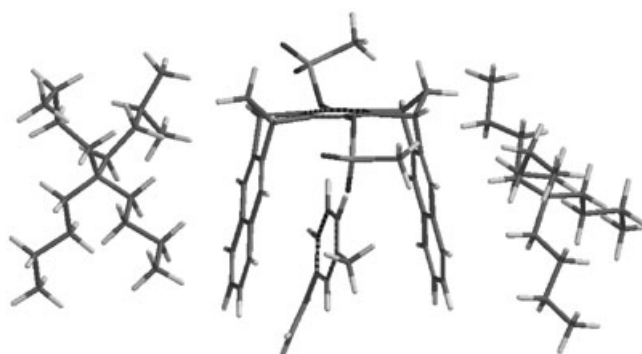


Figure 13. The lowest-energy structure of the complex **17-1a** including the tetra-*n*-butylammonium cations calculated by force-field AMBER*/H₂O with a Monte Carlo conformer search (MacroModel 6.5, 5000 structures).^[47,48]

of theory indicates that although its hydrophobic alkyl chains are calculated to aggregate with the outside of the naphthalene sidewalls of the clip, the position of the guest within the cavity of the clip seems to be only weakly influenced. Therefore, the complex structures were calculated in the following without the tetra-*n*-butylammonium cations at the force-field level. These are used as starting points for the quantum-chemical studies.

Starting from two lowest energy Amber*/H₂O structures, geometry optimizations were performed at the Hartree-Fock level (HF/6-31G**), with constraints on the guest position within the clip (Figure 14). Based on these structures the chemical shifts were computed by using gauge-including atomic orbitals (GIAO-HF) and SVP basis sets^[65] relative to the TMS reference computed at the same level. All quantum chemical calculations were performed with the program packages Q-Chem^[66] and TURBOMOLE.^[67] In the following, we consider only guest protons. The ^1H NMR complexation-induced chemical shieldings of NMNA-1 (see Figure 14), computed with the different structural parameters obtained with Amber*/H₂O and HF/6-31G**, differ by 0.4 ppm at most. Basis-set influences, determined by comparing the SVP basis with a TZP basis^[65] at the GIAO-HF level, are 0.1 ppm at most. This is consistent with previous studies on similar tweezer complexes, for which the accuracy of ^1H NMR chemical shifts computed at the GIAO-HF/SVP level on HF/6-31G* structures (as compared to calculations using electron correlation methods) was found to be in the order of 0.2–0.5 ppm.^[68–70] Complexation-induced shieldings are obtained as the difference of the chemical shifts for the bound and isolated guest (the structure of the isolated guest was optimized at the same level of theory) and are listed in Table 4. Computed and experimental relative NMR shieldings for the isolated nicotinamide **17** agree within 0.5 ppm. For host-guest complex NMNA-1 the maximum difference is 3.0 ppm, and for NMNA-2 2.1 ppm. For the complexation-induced chemical shieldings the difference between theory and experiment is reduced to 2.7 and 1.5 ppm for NMNA-1 and NMNA-2, respectively. Since the measurements were performed in water as solvent, a strong devia-

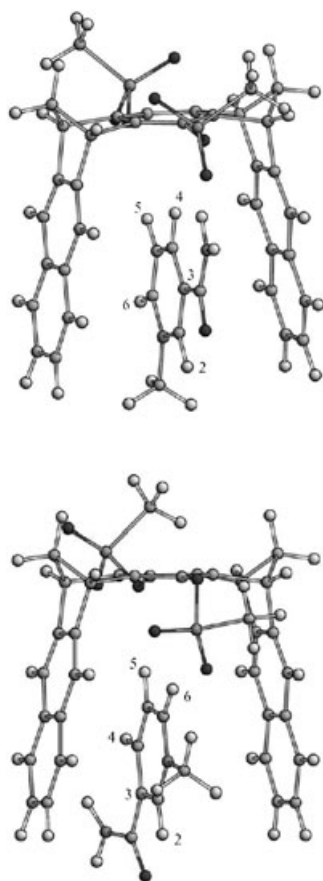


Figure 14. The lowest-energy AMBER*/H₂O structures of the complex **17-1a** optimized at HF/6-31G** level (with constraints): NMNA-1 (top) and NMNA-2 (bottom).

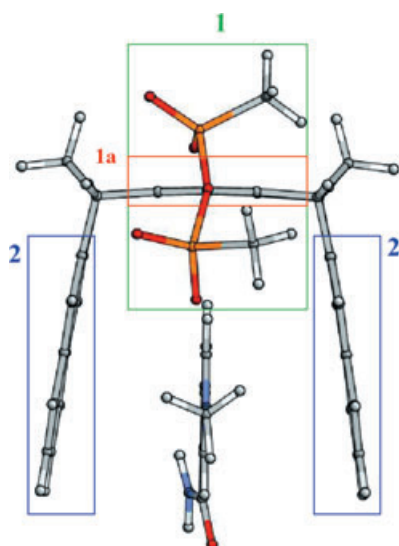


Figure 15. Partitioning of the clip within the NMNA-2 structure (AMBER*/H₂O). For part 1a the phosphonate groups (OP(CH₃)OO⁻) have been removed.

Table 4. Relative (δ) and complexation-induced ($\Delta\delta$) ¹H NMR chemical shifts [ppm] computed at the GIAO-HF/TZP level for the HF/6-31G** optimized *N*-methylnicotinamide host–guest structures NMNA-1 and NMNA-2 and the isolated guest structure **17** in comparison with the experimental results.

Proton	Isolated 17		17-1a				Exptl	
	Calcd δ	Exptl δ	NMNA-1 δ	$\Delta\delta$	NMNA-2 δ	$\Delta\delta$	δ	$\Delta\delta$
H2	9.8	9.3	7.8	2.0	7.1	2.7	8.3	1.2
H4	9.2	8.9	3.9	5.3	8.0	1.2	6.9	2.6
H5	8.2	8.2	5.8	2.4	6.5	1.7	6.4	2.3
H6	8.8	9.0	6.3	2.5	5.5	3.3	7.6	1.8

tion is not surprising. Besides structural flexibility, the influence of the water environment can be estimated to be on the order of at least 0.7 ppm for the aromatic guest protons of NMNA-1.^[71] This data was estimated by a preliminary simulation of the nicotinamide host–guest complex **17-1a** in a water environment by using a snapshot of a force-field molecular dynamics simulation with the water molecules closest to the center of the guest ring. We used the snapshot structure to compute the influence of the water molecules on the NMR shieldings explicitly at the GIAO-HF/6-31G** level for a system with up to 1003 atoms using our newly developed linear-scaling NMR chemical shift method.^[71] Clearly, for an accurate study of solvent effects a multitude of snapshots must be computed. Nevertheless, our calculations provide a first estimate. Further simulations are in progress. This indicates that the deviation between computed and measured complexation-induced shieldings of up to 2.7 ppm for the NMNA-1 structure seems to be larger than experimental and theoretical error bars, whereas the agreement for NMNA-2 is within the error bars.

Clip influences on ¹H NMR shifts of NMNA-2: In addition to the relative and complexation-induced chemical shieldings of **17-1a**, we studied the influence of different parts of clip **1a** on the ¹H NMR chemical shifts in the NMNA-2 structure. Therefore the clip was partitioned into three parts: 1) the upper unit including the phosphonate groups, 1a) the upper part without phosphonate groups, and 2) the naphthalene side walls (Figure 15, Table 5). Open bonds were saturated with protons (C–H 110 pm). The maximum influences of parts 1 and 2 are 0.7 and 4.3 ppm, respectively

Table 5. Influences of different parts of the clip on the relative chemical shifts [ppm] (GIAO-HF/SVP) of guest **17** in the NMNA-2 structure (see Figure 15) optimized at Amber*/H₂O force-field level.

Proton	δ_{isolated}	$\Delta_1^{[a]}$	$\Delta_2^{[a]}$	$\Delta_{1a}^{[a]}$	$\delta_{\text{isolated}} + \Delta_{1+2}^{[b]}$	$\delta_{\text{total}}^{[c]}$
H2	10.0	-0.7	-2.1	-0.3	7.2	7.5
H4	9.3	-0.5	-0.8	-0.3	8.0	8.2
H5	8.4	0.2	-1.7	-0.5	6.9	6.6
H6	9.2	-0.3	-4.3	-1.9	4.6	4.8

[a] Change in the chemical shifts of the isolated guest molecule due to the influence of parts 1, 2, and 1a of the clip. [b] Sum of Δ_1 and Δ_2 added to the chemical shifts for the isolated guest molecule. [c] Chemical shifts computed for the full host–guest complex.

(GIAO-HF/SVP at Amber*/H₂O structure). The maximum influence of part 1a of 1.9 ppm is stronger than that of part 1; this result indicates that the effects of the phosphonates and the ring currents are in opposite directions and lead to partial compensation. Overall the sum of the influences of parts 1 and 2 yields ¹H NMR shieldings for the guest protons that are in good agreement (within 0.3 ppm) with the full calculation. This indicates a weak influence of the linking units, as found similarly in other tweezer-shaped host-guest systems.^[70]

Computed ¹H NMR chemical shifts for 22-1a: Since for the NMNA-2 complex **17-1a** the influence on the ¹H NMR guest chemical shifts of the HF/6-31G** structure optimization was found to be quite small (less than 0.4 ppm) relative to those calculated with the Amber*/H₂O structure, the Amber*/H₂O structures (again resulting from a Monte Carlo conformer search) were used for the study of the NAD⁺ system **22-1a**. Although there is a multitude of possible host-guest structures, we consider here just two arrangements of NAD⁺ within the clip cavity, as shown in Figure 16: bound through the nicotinamide (NAD-1) and adenine parts (NAD-2). The corresponding computed NMR shieldings are listed in Table 6. The chemical shifts for the

Table 6. Relative (δ) and complexation-induced ($\Delta\delta$) ¹H NMR chemical shifts [ppm] computed at the GIAO-HF/SVP level on the Amber*/H₂O structures of the NAD⁺ host-guest complex: structures NAD-1 and NAD-2 and the isolated guest structure NAD⁺ (**22**) are compared to the experimental results.

Proton	Isolated NAD ⁺ (22)		22-1a				Exptl	
	Calcd δ	Exptl δ	NAD-2 δ	NAD-2 $\Delta\delta$	NAD-1 δ	NAD-1 $\Delta\delta$	δ	$\Delta\delta$
H2	9.0	9.4	8.4	0.6	7.6	1.4	9.0	0.4
H4	10.1	8.9	7.7	2.4	3.4	6.7	8.2	0.7
H5	8.5	8.3	7.3	1.2	6.1	2.4	7.5	0.8
H6	9.7	9.3	8.0	1.7	6.8	2.9	8.8	0.4
H7	8.4	8.6	5.8	2.6	7.6	0.8	8.2	0.3
H8	5.8	6.1	4.8	1.0	4.5	1.3	5.8	0.3
H9	5.5	6.2	5.4	0.1	5.5	0.0	5.9	0.2

isolated NAD⁺ guest **22** agree within 1.2 ppm with experiment, which is within the error bars of theory and experiment. As discussed above, relatively large theoretical error bars arise due to the missing solvent in the quantum chemical calculations. Comparison of the chemical shifts for NAD⁺ within the clip indicates that the NAD-1 structure leads to a difference of 4.8/6.0 ppm with respect to relative/complexation-induced chemical shieldings between theory and experiment. The second possible structure NAD-2 agrees better with the experiment: deviations are at most 2.4 and 2.3 ppm, respectively. Although this allows the NAD-1 structure to be discarded, no final and safe conclusion about how the adenine or nicotinamide moiety of NAD⁺ is bound to the clip can be drawn at this stage of our quantum chemical studies due to the multitude of possible structural arrangements. Here, further investigations are

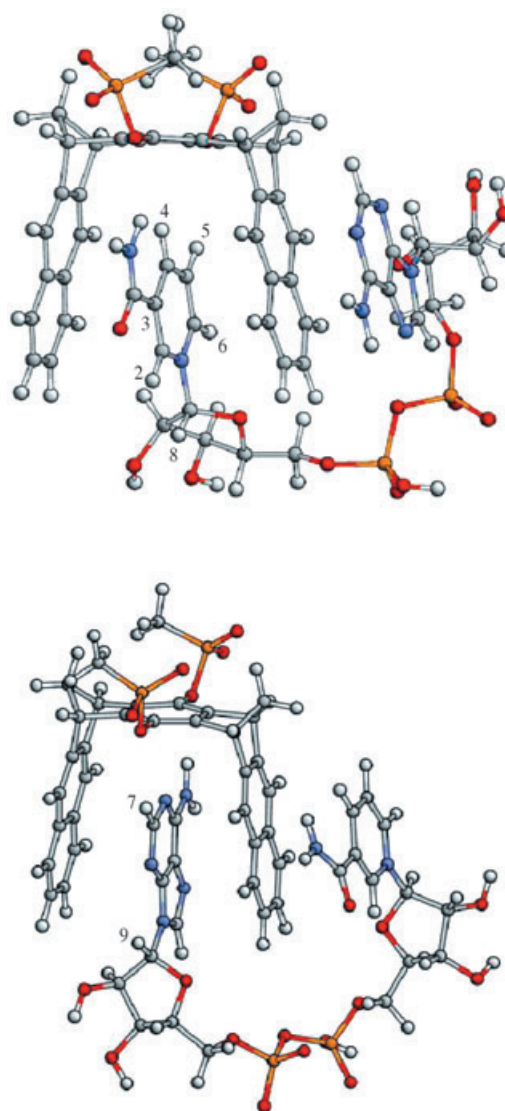


Figure 16. The lowest energy AMBER*/H₂O structures of the complex **22-1a**: NAD-1 (top: the nicotinamide ring inside the clip cavity) and NAD-2 (bottom: the adenine moiety inside the clip cavity).

planned, in particular with the smaller ribose-substituted systems such as 2'-desoxyadenosine (**24**), AMP (**25**), and NMN (**26**).

Energetics of NAD⁺ binding within clip 1a: In addition to the NMR considerations, we studied the binding energetics of NAD⁺ within the clip. For reliable results electron-correlation effects must be accounted for. We used the RI-MP2 approach (resolution of identity Møller–Plesset second-order perturbation theory)^[72] with an SVP basis set. All data are listed in Table 7. In a first step, we used for the computation of binding energies only the parts of NAD⁺ that are bound within the clip (free bonds were always saturated with protons, N–H 100 pm). Within the clip of charge –2 the nicotinamide part is bound by 152 kcal mol^{–1} in NAD-1 as compared to the adenine part bound with 37 kcal mol^{–1} in

Table 7. Influence of charge and guest structures on binding energies of NAD⁺ guest **22** within the clip **1a** computed at the RI-MP2/SVP level [in kcal mol⁻¹].

Clip 1a	Charge NAD ⁺ (22)	NAD-1	NAD-2
-2	+1 ^[a]	-151.7	-
-2	0 ^[a]	-46.4	-36.9
0	0 ^[a]	-34.1	-35.3
0	+1	-78.9	-71.1
0	0	-78.3	-70.8
-2	+1	-171.4	-144.3

[a] Only the part of the guest molecule bound inside the clip is considered (see text).

NAD-2. This is due to the positive charge of the nicotinamide unit. If this charge is neutralized, the nicotinamide binding energy decreases to 46 kcal mol⁻¹. This trend is reversed if the neutral guests are considered within a charge-neutralized clip (saturation with protons, O–H 96 pm), where adenine is slightly more strongly bound: 34 versus 35 kcal mol⁻¹. In the second step, we consider the full NAD⁺ guest (charge +1) within the clip with charge -2: binding through the nicotinamide unit leads to a stabilization energy of 171 kcal mol⁻¹, and binding through the adenine moiety to 144 kcal mol⁻¹. If all the charges are neutralized (which can be assumed to be more realistic for the system in water as solvent), the stronger stabilization of the nicotinamide versus adenine binding is much less pronounced: 78 versus 71 kcal mol⁻¹. Although it is clear that these energetics are highly influenced by structural changes and possibly also by methodological effects, they provide some insight into influences on the recognition process and suggest that both subunits are bound by the clip with a preference for the nicotinamide ring, in agreement with the experimental findings.

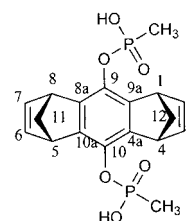
Conclusion

In this paper we have presented the water-soluble clip **1a** as a host molecule which binds *N*-alkylpyridinium ions and electron-poor aromatics highly selectively. The experimental results obtained for the complexation of the naturally occurring nucleosides or nucleotides **22–26** with **1a** and the quantum chemical calculations are good evidence for our assumption that NAD⁺ (**22**) and NADP (**23**) are indeed bound in a double complex geometry, in which either the pyridinium or the pyrimidine ring is inserted into the cavity of **1a**. A low-temperature NMR experiment should provide further insight into the dynamics of complexation. It would be interesting to examine whether at low temperatures the fast equilibrium between the complexed and free nicotinamide or adenine subunit is slowed down to below the NMR timescale and two isolated sets of signals appear. This experiment has been, however, prevented by the low solubility of the complex **22·1a** in CD₃OD, but it might be possible to measure the temperature dependence in a mixture of methanol and water, in which the complex is soluble (Sup-

porting Information, Figure S1). In the future, we will try to create highly selective NAD⁺ sensors using modified clips with built-in ribose recognition elements.^[73] Another important area is redox chemistry with NAD⁺. If the electrochemical potential of NAD⁺ is changed upon complexation, the substrate profile of dehydrogenases may be altered.^[74] Efficient trapping of NAD⁺ in enzymatic reductions may also lead to shifted equilibria or even ultimately reverse the course of the naturally occurring reaction. Finally, we intend to create artificial enzyme models with noncovalently bound zinc ions and complexed NAD⁺ without any protein present. In the future, we will carry out a systematic investigation on the inclusion properties of the other naturally occurring nucleosides. Binding of ATP or GTP might open new areas of interference in numerous biological pathways. It is also in principle conceivable that the well-preorganized clip is capable of a double intercalation mode into electron-poor base pairs of intact DNA.^[75,76] Any of these new interactions would render the bis-phosphonate clip a valuable new tool in DNA chemistry. Already our first prototype of a NAD⁺ or NADP binder, clip **1a**, can favorably compete with alcohol dehydrogenases for the oxidized form of their substrate: NAD⁺ is bound by the natural enzyme with *K_a* values around 10³ M⁻¹, in contrast to NADH which is grasped much more tightly (10⁵ M⁻¹). In the future, we wish to exploit this distinct *K_a* difference to interfere with enzymatic reductions.

Experimental Section

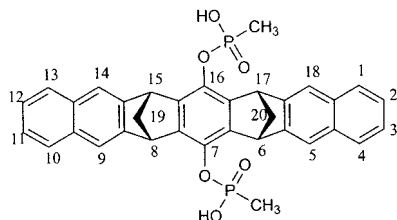
1,4,5,8-Tetrahydro-1,4:5,8-dimethanoanthracene-9,10-bismethylphosphonic acid ester (1b): The hydroquinone precursor^[58] (100 mg, 420 μmol) and methylphosphonic acid dichloride (150 mg 1.13 mmol, 2.7 equiv) were



dissolved in anhydrous THF (10 mL) and cooled to 0 °C. Then triethylamine (175 μL, 127 mg, 1.26 mmol, 3 equiv) was added dropwise, and a white solid precipitated after a few seconds. After 1 h, the precipitate was filtered off under argon, washed with a small amount of anhydrous THF, and the combined filtrates were treated with 2.5% aqueous HCl (3 mL). After 15 min of *n*-hexane (5 mL) was added, and the resulting two-layer system was stirred overnight, resulting in strong precipitation. The colorless solid was filtered off, washed with a little 2.5% aqueous HCl, and dried in vacuo to furnish 110 mg (279 μmol, 66%) of the bisphosphonate bismonoester as a colorless solid. M.p. decomp > 300 °C. ¹H NMR (300 MHz, [D₆]DMSO): δ = 1.48 (d, ²J(P,CH₃) = 17.1 Hz, 6H; CH₃), 2.10 (brs, 4H; 11-Hⁱ, 11-H^a, 12-Hⁱ, 12-H^a), 4.05 (brs, 4H; 1-H, 4-H, 5-H, 8-H), 6.75 ppm (brs, 4H; 2-H, 3-H, 6-H, 7-H); ¹³C NMR (50 MHz, [D₆]DMSO): δ = 12.42 (d, ¹J(P,C) = 139.2 Hz; CH₃), 47.90 (d, C-1, C-4, C-5, C-8), 69.50 (t, C-11, C-12), 136.53 (d, ³J(P,C) = 7.4 Hz; C-4a, C-8a, C-9a, C-10a), 142.32 (d, C-2, C-3, C-6, C-7), 142.92 ppm (d, C-9, C-10);

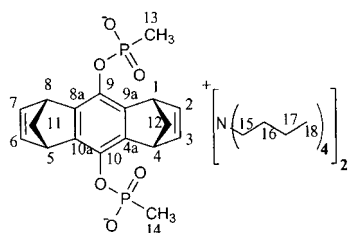
^{31}P NMR (81 MHz, $[\text{D}_6]\text{DMSO}$): $\delta = 29.86$ ppm (s); MS (ESI, MeOH): m/z : 196 $[\text{M}-2\text{H}^+]^{2-}$, 393 $[\text{M}-\text{H}^+]^-$, 425 $[\text{M}-\text{H}^++\text{MeOH}]^-$, 787 $[2\text{M}-\text{H}^+]^-$, 1181 $[3\text{M}-\text{H}^+]^-$; elemental analysis calcd (%) for $\text{C}_{18}\text{H}_{20}\text{P}_2\text{O}_6$: C 54.83, H 5.11; found: C 54.77, H 5.65.

6,8,15,17-Tetrahydro-6,17,8,15-dimethanoheptacene-7,16-bis(methylphosphonic acid ester) (1a): The hydroquinone precursor^[58] (100 mg,



228 μmol) and methylphosphonic acid dichloride (80 mg, 0.60 mmol, 2.7 equiv) were dissolved in anhydrous THF (10 mL) and cooled to 0°C . Then triethylamine (80 μL , 58.4 mg, 0.58 mmol, 3 equiv) was added dropwise, and a colorless solid precipitated after a few seconds. After 1 h, the solution was warmed to room temperature and stirred for another 1 h. The reaction mixture was quenched with 2.5% aqueous HCl (3 mL). After 20 min, *n*-hexane (5 mL) was added, and the resulting two-layer system was stirred overnight. Subsequently the aqueous layer was separated, the organic phase washed with 2.5% aqueous HCl (3 mL), and the combined organic phases evaporated to dryness on the rotavapor. Subsequent drying at 0.1 mbar and chromatographic purification over silica (300 \times 10 mm, gradient elution with CH_2Cl_2 :MeOH 3:1 \rightarrow 2:1) afforded 90 mg (0.15 mmol, 66%) of the phosphonate clip as a colorless solid. TLC: $R_f = 0.02$ (CH_2Cl_2 /MeOH 2:1); m.p. decomp $> 270^\circ\text{C}$; ^1H NMR (300 MHz, D_2O): $\delta = 1.49$ (d, $^2J(\text{PCH}_3) = 16.4$ Hz, 6H; PCH_3), 2.42 (dm, $^2J(19\text{-H}^i, 19\text{-H}^a) = 8.5$ Hz, 2H; 19-Hⁱ, 20-H), 2.66 (dm, $^2J(19\text{-H}^a, 19\text{-H}^i) = 8.3$ Hz, 2H; 19-H^a, 20-H^a), 4.69 (brs, 4H; 6-H, 8-H, 15-H, 17-H), 7.17 (ddm, $^3J(\text{H-1}, \text{H-2}) = 6.2$ Hz, $^4J(\text{H-4}, \text{H-2}) = 3.3$ Hz, 4H; 2-H, 3-H, 11-H, 12-H), 7.48 (ddm, $^3J(\text{H-2}, \text{H-1}) = 6.1$ Hz, $^4J(\text{H-2}, \text{H-4}) = 3.3$ Hz, 4H; 1-H, 4-H, 10-H, 13-H), 7.39 ppm (brs, 4H; 5-H, 9-H, 14-H, 18-H); ^{31}P NMR (81 MHz, D_2O): $\delta = 15.32$ ppm (s); MS (ESI, MeOH): m/z : 296 $[\text{M}-2\text{H}^+]^{2-}$, 593 $[\text{M}-\text{H}^+]^-$, 615 $[\text{M}-2\text{H}^++\text{Na}^+]^-$, 625 $[\text{M}-\text{H}^++\text{MeOH}]^-$.

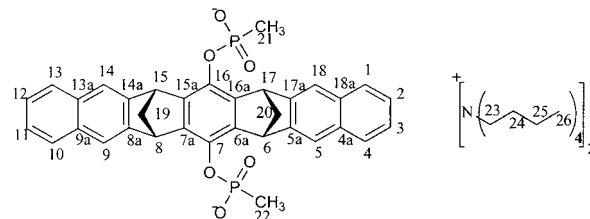
Bis(tetra-*n*-butylammonium) 1,4,5,8-tetrahydro-1,4:5,8-dimethanoanthracene-9,10-bismethylphosphonate (1d): The corresponding phosphonic acid **1b** (50 mg, 127 μmol) was suspended in dichloromethane (ca.



10 mL) and treated with aqueous tetra-*n*-butylammonium hydroxide (253 μL , 1 M, 253 μmol , 2.0 equiv). The mixture was stirred for 2 h at ambient temperature, and the solvent evaporated to dryness. Drying at 0.1 mbar afforded a quantitative yield of tetra-*n*-butylammonium salt **1d** as a colorless solid. M.p. 178°C ; ^1H NMR (300 MHz, $[\text{D}_4]\text{MeOH}$): $\delta = 1.03$ (t, $^3J(\text{CH}_2\text{CH}_3) = 7.3$ Hz, 24H; CH_2CH_3), 1.26 (d, $^2J(\text{PCH}_3) = 16.4$ Hz, 6H; PCH_3), 1.35–1.49 (m, 16H; CH_2CH_3), 1.60–1.74 (m, 16H; NCH_2CH_2), 2.15 (brs, 4H; 11-H, 12-H), 3.20–3.29 (m, 16H; NCH_2CH_2), 4.16 (brs, 4H; 1-H, 4-H, 5-H, 8-H), 6.79 ppm (brs, 4H; 2-H, 3-H, 6-H, 7-H); ^{13}C NMR (50 MHz, $[\text{D}_4]\text{MeOH}$): $\delta = 13.27$ (d, $^1J(\text{P,C}) = 136.5$ Hz; C-13, C-14), 13.93 (q, C-18), 20.73 (t, C-17), 24.79 (t, C-16), 59.51 (t, C-15), 70.63 (t, C-11, C-12), 139.62 (dd, $^3J(\text{P,C}) = 8.0$ Hz, $^4J(\text{P,C}) = 1.9$ Hz; C-4a,

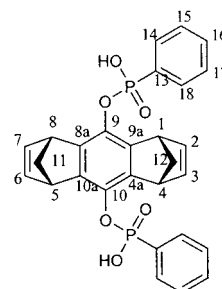
C-8a, C-9a, C-10a), 143.28 (m, C-2, C-3, C-6, C-7), 144.10 ppm (d, C-9, C-10); ^{31}P NMR (81 MHz, $[\text{D}_4]\text{MeOH}$): $\delta = 25.29$ ppm (s); MS (ESI, MeOH): m/z : 197 $[\text{M}-2\text{NBu}_4^+]^{2-}$, 415 $[\text{M}-2\text{NBu}_4^++\text{Na}^+]^-$, 425 $[\text{M}-2\text{NBu}_4^++\text{H}^++\text{MeOH}]^-$, 634 $[\text{M}-\text{NBu}_4^+]^-$; HRMS (ESI, MeOH): m/z : calcd for $\text{C}_{34}\text{H}_{54}\text{NP}_2\text{O}_6^- - \text{NBu}_4^+$: 634.342; found: 634.341.

Bis(tetra-*n*-butylammonium) 6,8,15,17-tetrahydro-6,17,8,15-dimethanoheptacene-7,16-bismethylphosphonate (1c): the respective phosphonic acid precursor **1a** (51.8 mg, 87.1 μmol), which contained small amounts



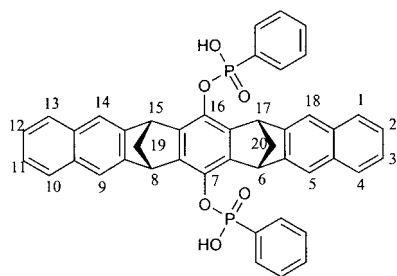
(ca. 5%) of silica gel, was suspended in dichloromethane (10 mL) and treated with aqueous tetra-*n*-butylammonium hydroxide (135 μL , 1 M, 135 μmol , 0.75 equiv). The mixture was stirred at room temperature for 2 h, and then the solvent was evaporated to dryness. The residue was redissolved in methanol and subsequently membrane-filtered and again evaporated to dryness. If the NMR analysis of this crude product indicated a small excess of tetra-*n*-butylammonium hydroxide, the product was again dissolved in methanol, and the phosphonic acid starting material (10 mg, 16.8 μmol) was added with vigorous stirring. A second membrane filtration, evaporation of the clear solution to dryness, and drying at 0.1 mbar furnished 59 mg (67.3 μmol , 99.7% with respect to the amount of tetra-*n*-butylammonium hydroxide) of clip **1c** as a light brown solid. M.p. 140°C ; ^1H NMR (300 MHz, $[\text{D}_4]\text{MeOH}$): $\delta = 0.96$ (t, $^3J(\text{CH}_2\text{CH}_3) = 7.3$ Hz, 24H; CH_2CH_3), 1.24–1.36 (m, 16H; CH_2CH_3), 1.40 (d, $^2J(\text{P-CH}_3) = 16.6$ Hz, 6H; P- CH_3), 1.43–1.56 (m, 16H; NCH_2CH_2), 2.37 (dm, $^2J(19\text{-H}^i, 19\text{-H}^a) = 8.0$ Hz, 2H; 19-Hⁱ, 20-H), 2.65 (dm, $^2J(19\text{-H}^a, 19\text{-H}^i) = 7.8$ Hz, 2H; 19-H^a, 20-H^a), 2.99–3.08 (m, 16H; NCH_2CH_2), 4.79 (brs, 4H; 6-H, 8-H, 15-H, 17-H), 7.19 (ddm, $^3J(\text{H-1}, \text{H-2}) = 6.1$ Hz, $^4J(\text{H-4}, \text{H-2}) = 3.2$ Hz, 4H; 2-H, 3-H, 11-H, 12-H), 7.54 (ddm, $^3J(\text{H-2}, \text{H-1}) = 6.1$ Hz, $^4J(\text{H-4}, \text{H-2}) = 3.2$ Hz, 4H; 1-H, 4-H, 10-H, 13-H), 7.59 ppm (brs, 4H; 5-H, 9-H, 14-H, 18-H). ^{13}C NMR (50 MHz, $[\text{D}_4]\text{MeOH}$): $\delta = 13.43$ (d, $^1J(\text{P,C}) = 137.2$ Hz; C-21, C-22), 13.90 (q, C-26), 20.59 (t, C-25), 24.64 (t, C-24), 59.33 (t, C-23), 65.77 (t, C-19, C-20), 120.82 (d, C-5, C-9, C-14, C-18), 125.96 (d, C-2, C-3, C-11, C-12), 128.62 (d, C-1, C-4, C-10, C-13), 133.51 (s, C-4a, C-9a, C-13a, C-18a), 142.09 (s, C-5a, C-8a, C-14a, C-17a), 148.91 ppm (d, C-7, C-16); the signals for C-6, C-8, C-15, C-17 are expected under the deuterium-coupled septet of $[\text{D}_4]\text{MeOH}$; the signals for C-6a, C-7a, C-15a, C-16a were too weak to be detected in $[\text{D}_4]\text{MeOH}$; ^{31}P NMR (81 MHz, $[\text{D}_4]\text{MeOH}$): $\delta = 25.29$ ppm (s); MS (ESI, MeOH): m/z : 296 $[\text{M}-2\text{NBu}_4^+]^{2-}$, 615 $[\text{M}-2\text{NBu}_4^++\text{Na}^+]^-$, 625 $[\text{M}-2\text{NBu}_4^++\text{H}^++\text{MeOH}]^-$, 834 $[\text{M}-\text{NBu}_4^+]^-$; HRMS (ESI, MeOH): m/z : calcd for $\text{C}_{50}\text{H}_{62}\text{NP}_2\text{O}_6^- - \text{NBu}_4^+$: 834.405; found: 834.407.

1,4,5,8-Tetrahydro-1,4:5,8-dimethanoanthracene-9,10-bis(phenylphosphonic acid ester) (2b): The hydroquinone precursor (100 mg, 420 μmol) and phenylphosphonic acid dichloride (117 μL , 164 mg, 841 μmol ,



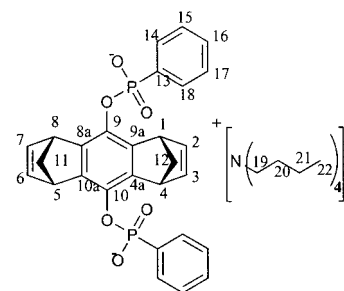
2.0 equiv) were dissolved in anhydrous THF (10 mL) and cooled to 0°C. Then triethylamine (175 µL, 1.26 mmol, 3 equiv) was added dropwise, and a white solid precipitated after a few seconds. After 1 h, the precipitate was filtered off under argon, washed with a little anhydrous THF, and the combined filtrates were treated with 2.5% aqueous HCl (3 mL). After 15 min, *n*-hexane (5 mL) was added, and the resulting two-layer system was stirred overnight, resulting in strong precipitation. The white solid was filtered off, washed with a little 2.5% aqueous HCl and dried in vacuo to furnish 110 mg (212 µmol, 50%) of the bis-phosphonate bis-monoester as a white solid. M.p. decomp at 290°C; ¹H NMR (300 MHz, [D₆]DMSO): δ = 1.82 (dm, ²J(12-Hⁱ, 12-H^a) = 6.9 Hz, 2H; 11-Hⁱ, 12-Hⁱ), 1.92 (dm, ²J(12-H^a, 12-Hⁱ) = 7.1 Hz, 2H; 11-H^a, 12-H^a), 3.79 (brs, 4H; 1-H, 4-H, 5-H, 8-H), 6.38 (brs, 4H; 2-H, 3-H, 6-H, 7-H), 7.44–7.63 (m, 6H; H_{ph}), 7.66–7.83 ppm (m, 4H; H_{ph}); ¹³C NMR (50 MHz, [D₆]DMSO): δ = 47.93 (d, C-1, C-4, C-5, C-8), 69.34 (t, C-11, C-12), 128.59 (d, ²J(P,C) = 14.8 Hz; C-14, C-14a, C-18, C-18a), 130.80 (d, ¹J(P,C) = 185.4 Hz; C-13, C-13a), 131.70 (d, ³J(P,C) = 9.7 Hz; C-15, C-15a, C-17, C-17a), 132.22 (m, C-16, C-16a), 136.50 (dd, ³J(P,C) = 7.9 Hz, ⁴J(P,C) = 2.3 Hz; C-4a, C-8a, C-9a, C-10a), 142.30 (m, C-2, C-3, C-6, C-7), 142.92 ppm (m, C-9, C-10); ³¹P NMR (81 MHz, [D₆]DMSO): δ = 17.45 ppm (s); MS (ESI, MeOH): *m/z*: 258 [M–2H⁺]²⁻, 539 [M–2H⁺+Na⁺]⁻, 517 [M–H⁺]⁻; elemental analysis calcd (%) for C₂₈H₂₄P₂O₆·2H₂O: C 60.43, H 5.43; found: C 60.37, H 5.10.

6,8,15,17-Tetrahydro-6,17,8,15-dimethanoheptacene-7,16-bis(phenylphosphonic acid ester) (2a): The hydroquinone precursor (100 mg, 228 µmol) was dissolved in anhydrous THF (10 mL) and cooled to 0°C. Then tri-



ethylamine (95 µL, 69.4 mg, 686 µmol, 3.0 equiv) and phenylhydrazine (55 µL) were added and stirred for 15 min, after which phenylphosphonic acid dichloride (100 µL, 140 mg, 718 µmol, 3.1 equiv) was added dropwise. After stirring for 3 h at room temperature, the precipitate was filtered off under argon, washed with a little anhydrous THF, and the combined filtrates were treated with 2.5% aqueous HCl (3 mL). After 15 min *n*-hexane (10 mL) was added, and the resulting two-layer system was stirred overnight. Subsequently, the aqueous layer was separated, the organic phase again washed with 2.5% aqueous HCl (3 mL), and the combined organic phases were dried with MgSO₄ and evaporated to dryness on a rotavapor. Subsequent drying at 0.1 mbar and chromatographic purification over silica (300 × 10 mm, elution with CH₂Cl₂/MeOH 3:1) afforded 40 mg (55.7 µmol, 24%) of the clip as a brown solid. TLC: R_f = 0.21 (CH₂Cl₂:MeOH 2:1); m.p. decomp at 295°C; ¹H NMR (300 MHz, D₂O): δ = 2.11 (dm, ²J(19-Hⁱ, 19-H^a) = 8.3 Hz, 2H; 19-Hⁱ, 20-Hⁱ), 2.24 (dm, ²J(19-H^a, 19-Hⁱ) = 8.3 Hz, 2H; 19-H^a, 20-H^a), 4.13 (brs, 4H; 6-H, 8-H, 15-H, 17-H), 7.22 (ddm, ³J(H-1, H-2) = 6.0 Hz, ⁴J(H-4, H-2) = 3.3 Hz, 4H; 2-H, 3-H, 11-H, 12-H), 7.39 (brs, 4H; 5-H, 9-H, 14-H, 18-H), 7.51 (ddm, ³J(H-2, H-1) = 6.0 Hz, ⁴J(H-2, H-4) = 3.3 Hz, 4H; 1-H, 4-H, 10-H, 13-H), 7.55–7.63 (m, 6H; H_{ph}), 7.80–7.88 ppm (m, 4H; H_{ph}); ¹³C NMR: could not be obtained due to poor solubility; ³¹P NMR (81 MHz, D₂O): δ = 15.32 ppm (s); MS (ESI, MeOH): *m/z*: 358 [M–2H⁺]²⁻, 717 [M–H⁺]⁻, 749 [M–H⁺+MeOH]⁻; HRMS (ESI, MeOH) calcd for C₄₄H₃₁P₂O₆⁻: 717.15959; found: 717.16184.

Bis(tetra-*n*-butylammonium) 1,4,5,8-tetrahydro-1,4:5,8-dimethanoanthracene-9,10-bisphenylphosphonate (2d): The corresponding phosphonic acid dihydrate **2a** (64.2 mg, 116 µmol) was suspended in dichloromethane



(ca. 10 mL), and was treated with aqueous tetra-*n*-butylammonium hydroxide (232 µL, 1 M, 232 µmol, 2.0 equiv). The mixture was stirred for 2 h at ambient temperature, and the solvent evaporated to dryness. Drying at 0.1 mbar afforded a quantitative yield of tetra-*n*-butylammonium salt **2d** as a brown solid. M.p. 184°C; ¹H NMR (300 MHz, [D₄]MeOH): δ = 1.02 (t, ³J(CH₂CH₃) = 7.3 Hz, 24H; CH₂CH₃), 1.34–1.49 (m, 16H; CH₂CH₃), 1.59–1.73 (m, 16H; NCH₂CH₂), 1.82 (brs, 4H; 11-H, 12-H), 3.18–3.29 (m, 16H; NCH₂CH₂), 3.74 (brs, 4H; 1-H, 4-H, 5-H, 8-H), 6.28 (brs, 4H; 2-H, 3-H, 6-H, 7-H), 7.28–7.44 (m, 6H; H_{ph}), 7.68–7.79 ppm (m, 4H; H_{ph}); ¹³C NMR (50 MHz, [D₄]MeOH): δ = 13.94 (q, C-22), 20.72 (t, C-21), 24.79 (t, C-20), 59.49 (t, C-19), 70.33 (t, C-11, C-12), 128.60 (d, ²J(P,C) = 13.7 Hz; C-14, C-14a, C-18, C-18a), 131.07 (m, C-16, C-16a), 133.26 (d, ³J(P,C) = 9.1 Hz; C-15, C-15a, C-17, C-17a), 137.02 (d, ¹J(P,C) = 177.38 Hz; C-13, C-13a), 139.48 (dd, ³J(P,C) = 8.0 Hz, ⁴J(P,C) = 1.9 Hz; C-4a, C-8a, C-9a, C-10a), 143.17 (m, C-2, C-3, C-6, C-7), 143.78 ppm (m, C-9, C-10); ³¹P NMR (81 MHz, [D₄]MeOH): δ = 14.25 ppm (s); MS (ESI, MeOH): *m/z*: 259 [M–2NBu₄⁺]²⁻, 517 [M–2NBu₄⁺+H⁺]⁻, 549 [M–2NBu₄⁺+H⁺+MeOH]⁻, 758 [M–NBu₄⁺]⁻; HRMS (ESI, MeOH): *m/z*: calcd for C₄₄H₃₈NP₂O₆⁻·NBu₄⁺: 758.37394; found: 758.36129.

NMR titrations: Ten NMR tubes were filled each with 0.6 mL of a solution of the host compound ([H] = 0.5–4 mM) in a deuterated solvent ([D₆]DMSO or CD₃OD). The guest compound G (about 1.5 equiv relative to the host) was dissolved in 0.61 mL of the same solvent, and the resulting solution was added with increasing volumes from 0 to 5 equiv to the host solution in ten NMR tubes. Volume and concentration changes were taken into account during analysis. The association constants were calculated by nonlinear regression methods [Eq. (1)] in which K = [H]₀/[G]₀.

$$\Delta\delta = \frac{\Delta\delta_{\max}}{2} \left(K + 1 + \frac{K}{[H]_0 K_a} - \sqrt{K^2 + \frac{2K_2}{[H]_0 K_a} - 2K + \frac{K^2}{[H]_0^2 K_a^2} + \frac{2K}{[H]_0 K_a} + 1} \right) \quad (1)$$

For dilution titrations equimolar amounts of host and guest compound were dissolved in deuterated methanol (0.5 mL) or water (0.5 mL) ([G] = [H] = 0.5–4 mM). From this reference sample, aliquots of 250, 125, 75, 50, and 25 µL were taken, and deuterated solvent was added to a total volume of 0.5 mL. Only those signals were used for quantitative evaluation which could be clearly detected during the whole titration. Binding constants K_a were determined by nonlinear regression.

Job plots: Equimolar solutions (10 mmol/10 mL, ca. 10 µM) of host and guest compound were prepared and mixed in various amounts. ¹H NMR spectra of the mixtures were recorded, and the chemical shifts were analysed by Job's method, modified for NMR data.

Salt-effect experiment: A dilution titration was carried out according to the general protocol outlined above (host and guest concentration: 10⁻⁴ M), but in the presence of 0.5 M aqueous tetra-*n*-butylammonium bromide. The change in chemical shifts became much smaller and the resultant binding constant from the nonlinear regression of the binding curves between host and *N*-methylnicotinamide dropped to almost zero (ca. 50 M⁻¹).

Microcalorimetry experiments: All titration experiments were performed on a TAM 2277 microcalorimeter (Thermometric, Järfälla, Sweden)

using the ampoule unit 2277-201. The temperature during the experiments was 298 K and we used water as solvent. 1 mL of the receptor solution was filled into the cell of the microcalorimeter. The substrate solution was added during the titration experiment by a syringe pump 6120-031 (Lund, Sweden).

Mass spectrometry: ESI mass spectra were recorded on a Finnigan MAT 95. Samples (20 μ L) were introduced as 10^{-5} M solutions in methanol at flow rates of 20 μ L min^{-1} . Heated capillary temperature: 150 °C. Ion spray potential: 3.5 kV (positive ESI), 3.0 kV (negative ESI). About 20–30 scans were averaged to improve the signal-to-noise ratio.

Simulation methods: Molecular mechanics calculations, Monte-Carlo simulations, and molecular dynamics: The program MacroModel 7.1 or 6.5^[47,48] was used for model building procedures and as graphical interface. Force-field parameters were taken from the built-in force fields, which were in some cases modified versions of the classical published versions. OPLS-AA and Amber* produced very similar results; the latter was subsequently chosen for all minimizations and Monte Carlo simulations. Minimizations were initially carried out in the gas phase, then in aqueous solution. Most complex structures were virtually identical under both conditions; this indicates strong enthalpic preference and hence stability of these arrangements. Energy minimizations were conducted over 1000 iterations on a Silicon Graphics O2 workstation or IBM workstation RS/6000 34P model 260. The best structures were subjected to conformational searches with 5000-step Monte Carlo simulations.

Acknowledgement

This work was supported by the DFG (Deutsche Forschungsgemeinschaft, Sonderforschungsbereich SFB 452) and the Fonds der Chemischen Industrie. C.O. acknowledges financial support by an Emmy Noether research grant of the DFG and the BMBF (Bundesministerium für Bildung und Forschung) within the “Zentrum für Multifunktionelle Werkstoffe und Miniaturisierte Funktionseinheiten” (BMBF 03N 6500). We thank Professor Monika Mazik (Universität Braunschweig) for her assistance with the interpretation of the calorimetric measurements.

- [1] D. Voet, J. G. Voet, *Biochemistry*, VCH, Weinheim, **1994**.
- [2] A. Fersht, *Enzyme Structure and Mechanism*, Freeman, New York, **1985**.
- [3] K. Dalziel, *The Enzymes Vol. XI*, Academic Press, New York, **1975**.
- [4] A. Wilkinson, J. Day, R. Bowater, *Mol. Microbiol.* **2001**, *40*, 1241–1248.
- [5] M. G. Rossmann, D. Moras, K. W. Olsen, *Nature* **1974**, *250*, 194–199.
- [6] A. M. Lesk, *Curr. Opin. Struct. Biol.* **1995**, *5*, 775–783.
- [7] C. A. Bottoms, P. E. Smith, J. J. Tanner, *Protein Sci.* **2002**, *11*, 2125–2137.
- [8] S. Ramaswamy, M. ElAhmad, O. Danielsson, H. Jornvall, H. Eklund, *Protein Sci.* **1996**, *5*, 663–671.
- [9] J. P. Gollivan, D. A. Dougherty, *J. Am. Chem. Soc.* **2000**, *122*, 870–874.
- [10] W. L. Zhu, X. J. Tan, C. M. Puah, J. D. Gu, H. L. Jiang, K. X. Chen, C. E. Felder, I. Silman, J. L. Sussman, *J. Phys. Chem. A* **2000**, *104*, 9573–9580.
- [11] S. Tsuzuki, M. Yoshida, T. Uchamaru, M. Mikami, *J. Phys. Chem. A* **2001**, *105*, 769–773.
- [12] S. Mecozzi, A. P. West, D. A. Dougherty, *J. Am. Chem. Soc.* **1996**, *118*, 2307–2308.
- [13] S. K. Burley, G. A. Petsko, *FEBS Lett.* **1986**, *203*, 139–143.
- [14] J. B. O. Mitchell, C. L. Nandi, I. K. McDonald, J. M. Thornton, S. L. Price, *J. Mol. Biol.* **1994**, *239*, 315–331.
- [15] S. Karlin, M. Zuker, L. Brocchieri, *J. Mol. Biol.* **1994**, *239*, 227–248.
- [16] A. M. de Vos, M. Ultshc, A. A. Kossiakoff, *Science* **1992**, *255*, 306–312.
- [17] O. Livnah, E. A. Stura, D. L. Johnson, S. A. Middleton, L. S. Mulcahy, N. C. Wrighton, W. J. Dower, L. K. Jolliffe, I. A. Wilson, *Science* **1996**, *273*, 464–471.
- [18] D. A. Dougherty, H. A. Lester, *Nature* **2001**, *411*, 252–254.
- [19] K. Brejc, W. J. van Dijk, R. V. Klaassen, M. Schuurmans, J. van der Oost, A. B. Smit, T. K. Sixma, *Nature* **2001**, *411*, 269–276.
- [20] J. C. Ma, D. A. Dougherty, *Chem. Rev.* **1997**, *97*, 1303–1324.
- [21] D. A. Dougherty, *Science* **1996**, *271*, 163–168.
- [22] H.-J. Schneider, T. Schiestel, P. Zimmerman, *J. Am. Chem. Soc.* **1992**, *114*, 7698–7703.
- [23] H. J. Schneider, *Chem. Soc. Rev.* **1994**, *23*, 227–234.
- [24] M. Dhaenens, L. Lacombe, J.-M. Lehn, J.-P. Vigneron, *J. Chem. Soc. Chem. Commun.* **1984**, 1097–1099.
- [25] R. Meric, J. P. Vigneron, J. M. Lehn, *J. Chem. Soc. Chem. Commun.* **1993**, 129–131.
- [26] H. J. Schneider, R. Kramer, S. Simova, U. Schneider, *J. Am. Chem. Soc.* **1988**, *110*, 6442–6448.
- [27] K. Araki, H. Shimizu, S. Shinkai, *Chem. Lett.* **1993**, 205–208.
- [28] K. Murayama, K. Aoki, *Chem. Commun.* **1997**, 119–120.
- [29] L. Garel, B. Lozach, J. P. Dutasta, A. Collet, *J. Am. Chem. Soc.* **1993**, *115*, 11652–11653.
- [30] S. Kubik, *J. Am. Chem. Soc.* **1999**, *121*, 5846–5855.
- [31] S. M. Ngola, P. C. Kearney, S. Mecozzi, K. Russell, D. A. Dougherty, *J. Am. Chem. Soc.* **1999**, *121*, 1192–1201.
- [32] S. Rensing, M. Arendt, A. Springer, T. Grawe, T. Schrader, *J. Org. Chem.* **2001**, *66*, 5814–5821.
- [33] T. J. Shepodd, M. A. Petti, D. A. Dougherty, *J. Am. Chem. Soc.* **1988**, *110*, 1983–1985.
- [34] A. Schenning, B. Debruin, A. E. Rowan, H. Kooijman, A. L. Spek, R. J. M. Nolte, *Angew. Chem.* **1995**, *107*, 2288–2289; *Angew. Chem. Int. Ed. Engl.* **1995**, *34*, 2132–2134.
- [35] D. Philp, J. F. Stoddart, *Angew. Chem.* **1996**, *108*, 1242–1286; *Angew. Chem. Int. Ed. Engl.* **1996**, *35*, 1154–1196.
- [36] M. Lamsa, J. Huuskonen, K. Rissanen, J. Pursiainen, *Chem. Eur. J.* **1998**, *4*, 84–92.
- [37] A. E. Rowan, J. Elemans, R. J. M. Nolte, *Acc. Chem. Res.* **1999**, *32*, 995–1006.
- [38] J. Elemans, M. B. Claase, P. P. M. Aarts, A. E. Rowan, A. Schenning, R. J. M. Nolte, *J. Org. Chem.* **1999**, *64*, 7009–7016.
- [39] F. P. Schmidtchen, *Chem. Ber.* **1981**, *114*, 597–607.
- [40] H. Fenniri, M. W. Hosseini, J. M. Lehn, *Helv. Chim. Acta* **1997**, *80*, 786–803.
- [41] A. Domenech, E. Garcia-Espana, J. A. Ramirez, B. Celda, M. C. Martinez, D. Monleon, R. Tejero, A. Bencini, A. Bianchi, *J. Chem. Soc. Perkin Trans. 2* **1999**, 23–32.
- [42] F. G. Klärner, B. Kahlert, *Acc. Chem. Res.* **2003**, *36*, 919–932.
- [43] F.-G. Klärner, J. Benkhoff, R. Boese, U. Burkert, M. Kamieth, U. Naatz, *Angew. Chem.* **1996**, *108*, 1195–1198; *Angew. Chem. Int. Ed. Engl.* **1996**, *35*, 1130–1133.
- [44] F. G. Klärner, J. Polkowska, J. Panitzky, U. P. Seelbach, U. Burkert, M. Kamieth, M. Baumann, A. E. Wigger, R. Boese, D. Bläser, *Eur. J. Org. Chem.* **2004**, 1405–1423.
- [45] M. Herm, O. Molt, T. Schrader, *Chem. Eur. J.* **2002**, *8*, 1485–1499.
- [46] C. Jasper, T. Schrader, J. Panitzky, F.-G. Klärner, *Angew. Chem.* **2002**, *114*, 1411–1415; *Angew. Chem. Int. Ed.* **2002**, *41*, 1355–1358.
- [47] F. Mohamadi, N. G. J. Richards, W. C. Guida, R. Liskamp, M. Lipton, C. Caufield, G. Chang, T. Hendrickson, W. C. Still, *J. Comput. Chem.* **1990**, *11*, 440–467.
- [48] MacroModel, v. 7.1, Schrödinger, 1500 SW First Ave., Ste. 1180, Portland, OR 97201.
- [49] C. S. Wilcox, *Frontiers in Supramolecular Chemistry, Photochemistry*, VCH, Weinheim, **1991**.
- [50] L. Fielding, *Tetrahedron* **2000**, *56*, 6151–6170.
- [51] We would like to thank Prof. H. J. Schneider for a copy of his program for 1:1 complexes. Binding constants were determined with Sigma Plot 3.02 from Jandel Corporation.
- [52] P. Job, *C. R. Hebd. Seances Acad. Sci.* **1925**, *180*, 925.
- [53] K. A. Connors, *Binding Constants, The Measurement of Molecular Complex Stability*, Wiley, New York, **1987**.

- [54] M. T. Blanda, J. H. Horner, M. Newcomb, *J. Org. Chem.* **1989**, *54*, 4626–4636.
- [55] S. L. Tobey, E. V. Anslyn, *J. Am. Chem. Soc.* **2003**, *125*, 10963–10970.
- [56] M. Berger, F. P. Schmidtchen, *Angew. Chem.* **1998**, *110*, 2840–2842; *Angew. Chem. Int. Ed.* **1998**, *37*, 2694–2696.
- [57] P. J. Garratt, A. J. Ibbett, J. E. Ladbury, R. O'Brien, M. B. Hursthouse, K. M. A. Malik, *Tetrahedron* **1998**, *54*, 949–968.
- [58] F.-G. Klärner, J. Panitzky, D. Blaser, R. Boese, *Tetrahedron* **2001**, *57*, 3673–3687.
- [59] E. A. Meyer, R. K. Castellano, F. Diederich, *Angew. Chem.* **2003**, *115*, 1244–1287; *Angew. Chem. Int. Ed.* **2003**, *42*, 1210–1250.
- [60] C. Tanford, *The Hydrophobic Effect*, Wiley, New York, **1980**.
- [61] W. Blokzijl, J. Engberts, *Angew. Chem.* **1993**, *105*, 1610–1648; *Angew. Chem. Int. Ed. Engl.* **1993**, *32*, 1545–1579.
- [62] N. Muller, *Acc. Chem. Res.* **1990**, *23*, 23–28.
- [63] T. Lazaridis, *Acc. Chem. Res.* **2001**, *34*, 931–937.
- [64] This may have two reasons: 1) The distance between the pyridinium cation and the embracing walls is still too large for van der Waals contact; 2) the HOMO–LUMO gap between the naphthalene donor and the pyridinium donor is too large.
- [65] A. Schäfer, H. Horn, R. Ahlrichs, *J. Chem. Phys.* **1992**, *97*, 2571.
- [66] J. Kong, C. A. White, A. I. Krylov, D. Sherrill, R. D. Adamson, T. R. Furlani, M. S. Lee, A. M. Lee, S. R. Gwaltney, T. R. Adams, C. Ochsenfeld, A. T. B. Gilbert, G. S. Kedziora, V. A. Rassolov, D. R. Maurice, N. Nair, Y. H. Shao, N. A. Besley, P. E. Maslen, J. P. Dombroski, H. Daschel, W. M. Zhang, P. P. Korambath, J. Baker, E. F. C. Byrd, T. Van Voorhis, M. Oumi, S. Hirata, C. P. Hsu, N. Ishikawa, J. Florian, A. Warshel, B. G. Johnson, P. M. W. Gill, M. Head-Gordon, J. A. Pople, *J. Comput. Chem.* **2000**, *21*, 1532–1548.
- [67] R. Ahlrichs, M. Bär, M. Häser, H. Horn, C. Kölmel, *Chem. Phys. Lett.* **1989**, *162*, 165.
- [68] C. Ochsenfeld, *Phys. Chem. Chem. Phys.* **2000**, *2*, 2153–2159.
- [69] S. P. Brown, T. Schaller, U. P. Seelbach, F. Koziol, C. Ochsenfeld, F.-G. Klärner, H. W. Spiess, *Angew. Chem.* **2001**, *113*, 740–743; *Angew. Chem. Int. Ed.* **2001**, *40*, 717–720.
- [70] C. Ochsenfeld, F. Koziol, S. P. Brown, T. Schaller, U. P. Seelbach, F.-G. Klärner, *Solid State Nucl. Magn. Reson.* **2002**, *22*, 128–153.
- [71] C. Ochsenfeld, J. Kussmann, F. Koziol, *Angew. Chem.* **2004**, *116*, 4585–4589; *Angew. Chem. Int. Ed.* **2004**, *43*, 4485–4489.
- [72] K. Eichkorn, O. Treutler, H. Öhm, M. Häser, R. Ahlrichs, *Chem. Phys. Lett.* **1995**, *240*, 283–289.
- [73] T. D. James, K. Sandanayake, S. Shinkai, *Angew. Chem.* **1996**, *108*, 2038–2050; *Angew. Chem. Int. Ed. Engl.* **1996**, *35*, 1910–1922.
- [74] The natural redox potential has the following value: $E^0 = -0.315 \text{ V}^{[1]}$ Inside the clip, it will most probably be lowered.
- [75] L. S. Lerman, *J. Mol. Biol.* **1961**, *3*, 18.
- [76] K. E. Erkkila, D. T. Odom, J. K. Barton, *Chem. Rev.* **1999**, *99*, 2777–2795.

Received: June 15, 2004
Published online: November 24, 2004